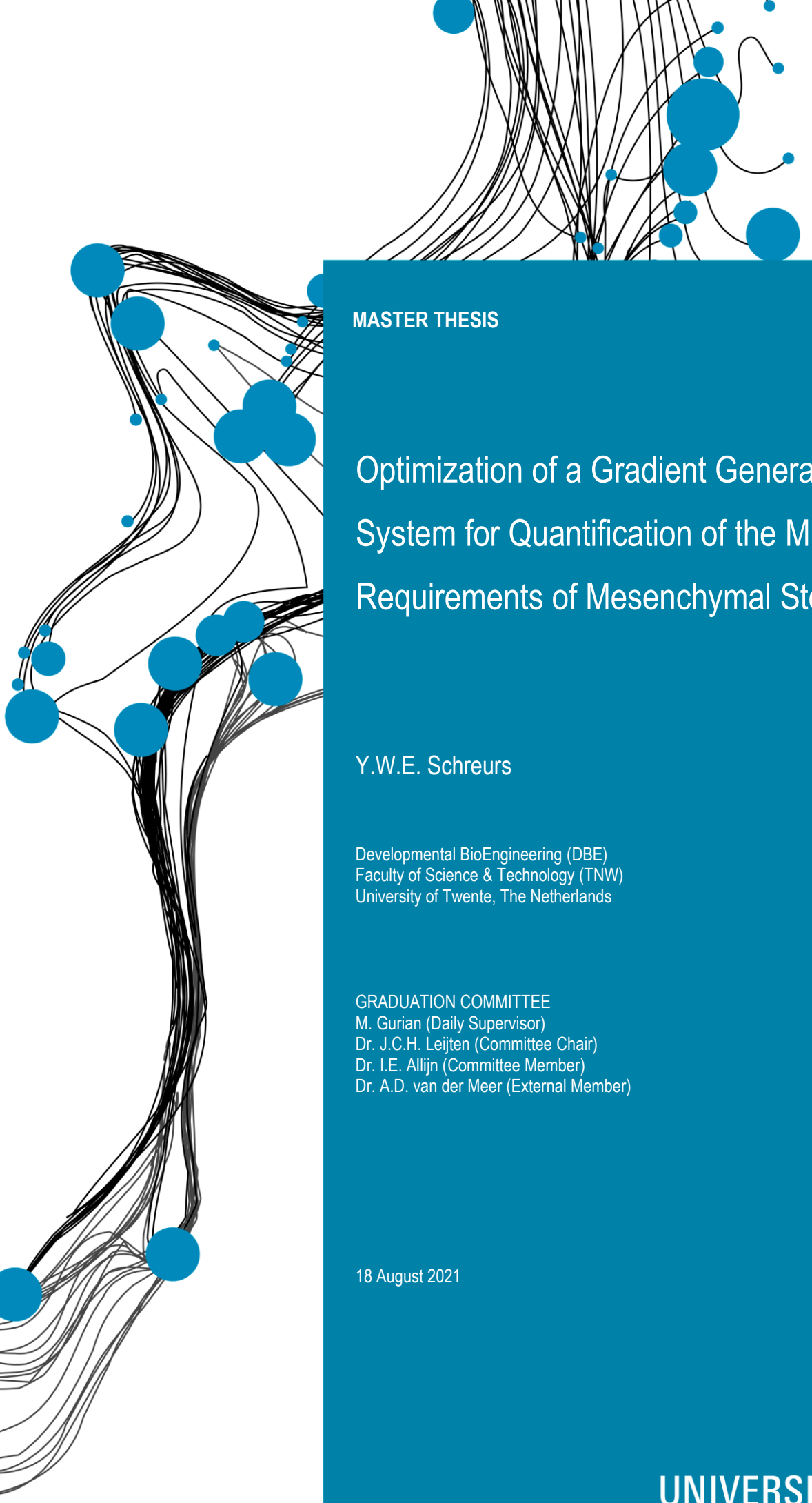

MASTER THESIS

Optimization of a Gradient Generating Microfluidic System for Quantification of the Minimal Metabolic Requirements of Mesenchymal Stem Cells in Anoxia

Y.W.E. Schreurs

Developmental BioEngineering (DBE)
Faculty of Science & Technology (TNW)
University of Twente, The Netherlands

GRADUATION COMMITTEE
M. Gurian (Daily Supervisor)
Dr. J.C.H. Leijten (Committee Chair)
Dr. I.E. Allijn (Committee Member)
Dr. A.D. van der Meer (External Member)

18 August 2021

UNIVERSITY OF TWENTE.

Acknowledgements

First of all, I would like to thank Melvin Gurian for his support and supervision during this project. He helped me to be critical about everything and we had many useful discussions. Moreover, he was extremely understanding when I wasn't able to work full-time on this project. The continuous supervision during my project by Jeroen Leijten was very much appreciated and I gained some very useful insights during our meetings. Furthermore I would like to thank Iris Allijn for sharing her knowledge and taking place in my graduation committee. Moreover, I want to thank Carlo Paggi for helping me out in the lab on many occasions. Next, I would like to thank Andries van der Meer for taking place in my graduation committee, for his interest in the project, and for evaluating the thesis.

Finally, I would like to thank my family, friends, and fellow students for all the support and laughs during this project.

Abstract

Tissue regeneration is an up and coming field within the life sciences with drastically increasing investigations regarding repair or replacement of damaged or missing tissue. One of the main challenges within tissue engineering is the unification of the foreign material, incorporated with hMSCs, with the donor site. The origin of this problem is the lack of vascularization at the donor site which results in an anoxic core in the implant, which turns necrotic. This project aims to optimise a gradient generating microfluidic system. This system will eventually be used to obtain data on the minimal metabolic requirements of hMSCs in anoxia. With this data hMSCs incorporated in implants can be supplied with sufficient metabolites to survive the period in which it is not yet connected to the donor site.

This dynamic system is optimised with the use of 3T3 cells by tuning several variables within the set up, such as the chip design, tubing, and flow rate. Biological variables within the system have been optimised with hMSCs in a static environment and tested in the dynamic set up. These variables include but are not limited to; coating, donor, and medium. The effect on the hMSCs is assessed with live/dead assays, PrestoBlue assays, and visual observations.

A stable gradient generating microfluidic system is optimised, in which several concentrations of metabolites can be tested for their effect on hMSCs in anoxia. An important variable within the system is the choice of hMSC donor, on which the functionality of the system depends. With this system a data set can be constructed on the minimal metabolic requirements for hMSCs in anoxia and provide a stepping stone for future work with hMSCs in tissue engineered constructs regarding metabolism.

List of abbreviations

2D	Two-dimensional
3T3	Mouse embryonic fibroblasts
aMEM	alpha-Minimum Essential Medium
AsAP	Ascorbic acid 2 phosphate
ATP	Adenosine triphosphate
BMP	Bone morphogenetic protein
COL	Collagen-I
DAB	Diaminobenzidine
DMEM	Dulbecco's Minimum Essential Medium
EC	Endothelial cell
ECM	Extra-cellular matrix
$FADH_2$	Flavine-adenine-dinucleotide
FBS	Fetal bovine serum
FEP	Fluorinated ethylene propylene
FGF	Fibroblast growth factor
FSS	Fluorescein sodium salt
G6P	glucose 6-phosphate
GOx	Glucose oxidase
HCl	Hydrochloride
HIF-1α	Hypoxia-inducible factor-1α
hMSC	Human mesenchymal stem cell
HRP	Horseradish peroxidase
HUVEC	Human umbilical vein endothelial cell
ID	Inner diameter
IGF	Insulin-like growth factor
ITS	Insulin-transferrin-selenium
mQ	Milli-Q water
NADH	Nicotinamide-adenine-dinucleotide
NADPH	Nicotinamide-adenine-dinucleotidephosphate
NaHCO3	Sodium bicarbonate
OD	Outer diameter
PBS	Phosphate-buffered saline
PD	Polydopamine
PDMS	Polydimethylsiloxane
pen/strep	Penicillin Streptomycin
PPP	Pentose phosphate pathway
qPCR	quantitative Polymerase Chain Reaction
R5P	ribose-5-phosphate
SFM	Serum-free medium
TCA-cycle	Tricarboxylic acid cycle
TFC	Theoretical fluorescence concentration
Tris	Trizma® base
VEGF	Vascular endothelial growth factor

Contents

1 Introduction

1.1 Tissue engineering

Daily, thousands of surgical procedures are performed to save and improve the quality of life, by repairing or replacing damaged tissue.[1] Some of the first mentions of these kinds of procedures were intended to replace entire body parts, such as dental implants made of shells, gold or ivory. [105] In more recent history these implants have become more and more advanced with the development and implementation of full joint implants made from metals, polymers, or any combination of these. With the implementation of an increasing number of materials within the body, material-body reactions have to be taken into account, since these can trigger an immune response, encapsulating the implant, resulting in a non-functional implant. Failing implants can moreover be due to the release of toxic quantities of particles, or implants can break as a whole. [2; 3]

Tissue engineering, dedicated to the generation of new tissue with a combination of engineering and biological principles are however quite more recent. An often applied example of tissue engineering are autografts, where a certain kind of tissue from the patient is moved to the site of injury on its body. Some of the benefits of this procedure are the use of a healthy living tissue and small chances of disease transmission.[4] The main limitation with autografts is the limited volume of tissue which can be taken from a healthy part to not interfere with its function.[5]

Another approach is the implementation of for example the use of cell-free bovine extracellular matrix (ECM) in implants. This method is used for differentiation of implemented cells toward the desired tissue and for the biological characteristics of this ECM such as cell attachment. However, due to the difficulty reproducing and controlling these materials as well as the potential disease transmission, the use of bovine ECM raises several concerns for its clinical application.[6] Due to the decrease in possible complications such as encapsulation or failure of the implant, via the implementation of such biological solutions, an increase of interest in this multidisciplinary field is observed. Although these biological solutions showed some promising results in the past, the main restraint is the possibility of only being of use at a small scale (several mm^3). [7; 8]

The limitations within the existing methods increase the demand for effective tissue engineering approaches. With these approaches, researchers aim to develop engineering and biological solutions for problems which cannot be solved without the combination of these biological and engineering approaches. This current approach is multidisciplinary, for tissue engineering this means a combination of cells, growth factors, and scaffolds are used to replace, repair or regenerate lost or damaged tissue. A wide variety of scaffolds, from naturally derived matrices to synthetic polymers, and growth factors, such as BMP's, IGF, and FGF, are used, depending on the target tissue. [1; 9; 10] The cells often used for these solutions are human mesenchymal stem cells (hMSCs), as they offer pluripotent and self renewal properties.

hMSCs have shown to be a promising therapy in regenerative medicine research and current clinical trials use hMSCs for tackling a wide variety of diseases regarding the musculoskeletal system, nervous system, cardiovascular, haematological, and many others. From these studies, hMSCs have grown to be widely accepted within the biomedical field as a key factor within several medical approaches and not only for stem cell therapy.[11; 12; 13]

Moreover, hMSCs secrete trophic factors, such as proangiogenic factors, in an intricately controlled way. These factors are especially interesting as they enhance vascularization of implanted engineered

tissues, ensuring complete integration into the host.[14; 15] Angiogenesis, which is the ischaemia- or hypoxia-driven formation of vasculature, is a key factor within tissue engineering. This vasculature is responsible for the delivery of oxygen and nutrients to the tissue and drainage of waste products, needed for proper functioning of tissue. Without these properties, a lack of oxygen and nutrients will co-exist with an accumulation of waste products, eventually leading to a dysfunctional tissue with a high level of cell death. [16; 17]

Currently, functional tissue engineered constructs have been successfully created, implanted and incorporated in small animals such as mice, for several different medical applications. For example for urinary diversion several biomaterials are tested on animals of different sizes, from rats to pigs, where different animal models are used for different disease profiles.[18] Moreover, *Lee et. al.* developed a PCL nanosheet seeded with muscle-derived stem cells to replace a conventional ileal conduit in rats and indicated skeletal muscle differentiation and growth into the PCL sheet.[19] With a study by *Oryan and Alidadi*, a large bone defect in rabbits was successfully repaired using the biodegradable biomaterial calcium silicate/chitosan, which resulted in a high level of bone formation and biomechanical performance.[20]

From these examples of successful incorporation of tissue engineered constructs in small animals, it can be stated the general idea of implanting engineered tissues seem to work. However, due to the shear size difference between these small constructs (0,5-20 mm^3) and clinically relevant sized constructs (0.1-10cm^3), current successful solutions are often not clinically relevant for human application. This is why these successful engineered constructs are being to scaled up, but it has proven to be challenging and remains an unresolved issue, since upscaling of TE constructs faces several problems.[7; 8; 21]

1.1.1 Problem of scaling up

Scaling up a living tissue engineered construct from roughly a couple mm^3 in size to a construct of several cm^3, gives rise to multiple problems. When implanting a living tissue, even in the most optimal conditions it does not connect to the implant site directly, but it rather takes weeks to form vascularization, needed for the oxygen and nutrient delivery the implant depends on for its survival.[17] For oxygen to still reach cells away from vasculature, it fully depends on diffusion, which is limited to 100-200 μm *in vivo*, depending on the tissue.[22; 16] As a result of this, an oxygen and nutrient depleted environment will be established in which the MSCs are situated. This explains the current successful implanted constructs to be mainly very thin or avascular tissue, such as skin or cartilage.[23]

This oxygen diffusion limit leads to an oxygen gradient within the tissue construct, as the one in figure 1, from normoxic conditions on the edge, mild hypoxia, to an anoxic region deeper into the tissue. The cells on the edge of the construct take up oxygen, disregarding the needs of the rest of the construct, leading to a vast decrease in oxygen availability when moving deeper into the tissue.[24] Not only do the anoxic regions cause necrosis of the tissue, the oxygen gradient could result in irregular cell differentiation and function.[25]

Oxygen plays a large role in cell survival due to the oxygen dependent metabolic pathways, which result in effective ATP production, which can be used for proliferation and differentiation of the cells. The switch to an hypoxic cell environment asks for a metabolic switch with the aim on cell preservation instead of proliferation, resulting in a less efficient ATP production.[26; 27]

Not only oxygen has a diffusion limit but nutrients as well, for nutrients the consumption by the cells and relatively slow supply result of a limit of 200 μm. This limit causes a nutrient deficiency for

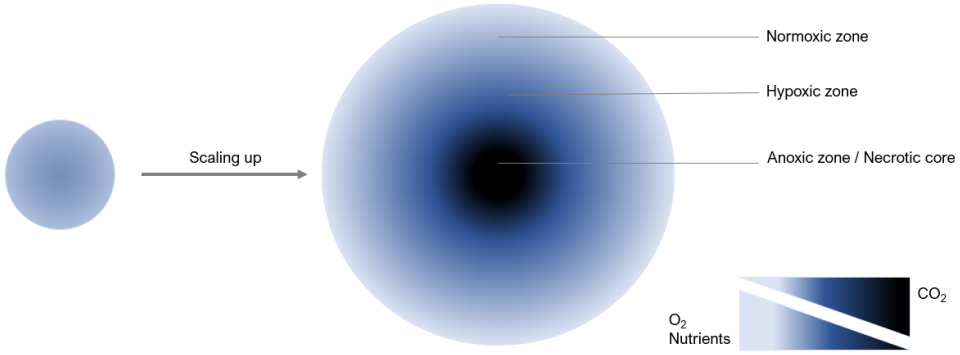

Figure 1: *Schematic example of necrotic core formation in a tissue after scaling up, as opposed to the small tissue, with a decreasing gradient of oxygen and nutrient supply and an increase in CO_2 towards the centre*

cells which are further from the implant surface. Just as with oxygen, a gradient of nutrient supply will result in decreased tissue functionality due to non-uniform cell differentiation and cell death. Next to the non-uniformity of the tissue, the oxygen and nutrient gradient can result in a necrotic core as is shown in figure 1. [24]

Current approaches to protect the MSCs from cell death due to these harsh *in vivo* conditions, describe the use of fetal bovine serum (FBS) in the production process. These results are promising, but serious questions arise regarding the use of FBS in clinical trials, due to the high variation between batches, unidentified factors, and possible cross contamination of animal diseases. [14; 28] One way to avoid the use of FBS, is serum free medium (SFM), also called xeno-free media, or chemically defined media. SFM has been optimised for the use of various cell types and its use can lead to a more consistent production of homogeneous MSCs populations, which are less affected by these harsh conditions. [29]

1.2 State of the art

Tissue engineering is an emerging field within the medical sciences, and multiple facets, such as vascularization and oxygenation are currently being extensively explored. The goal of these methods is to improve the success rates of these tissue engineered constructs, which are increasing in size.

1.2.1 Vascularization

Within tissue engineering, vascularization is a key challenge which is currently hindering clinical applications. Vascularization is important for the oxygenation of tissue, supplying tissue with nutrients, and draining tissue of waste products. Ideally, a tissue engineered construct will be supplied with a complete vasculature, perfectly connecting to the existing vasculature of the implant site. This way the newly implanted tissue engineered construct can profit directly from the waste drainage and supply of oxygen and nutrients. Fundamental elements for the formation of new vasculature are endothelial cells (ECs), angiogenic factors, biophysical cues, and spatial organisation.[8] *In vivo* vascularization, as a result of hypoxia, is started by angiogenic factors, such as VEGF, secreted by the nutrient-deprived, hypoxic micro environments. Angiogenesis in such an environment is especially important for growth and function of the tissue. [30] Quiescent ECs are activated by the angiogenic factors and allow a tip cell to migrate to the source of the signal. Next to the tip cell, stalk cells will emerge, proliferating for sprout elongation and forming the start of the lumen. [8; 31][77(p.1236)] This connection of the implant to the body without interference takes several weeks, due to the vasculature forming at a speed of several tenths of

μm per day.

Current approaches for vascularization are stimulation of angiogenesis via cell free approaches; e.g. growth factors, via cell therapy approaches; e.g. implementation of HUVECs, and prevascularization of the construct, either mechanical (via 3D printing) or biological. [32]

Although these approaches are quite promising as medium to long term solutions, on the short term, they are not as successful, since time is still necessary to connect the implant to the receiving end, leaving the cells with an accumulation of waste products and shortage of nutrients.[17]

1.2.2 Oxygenation

With oxygenation, materials are incorporated within the construct which release oxygen, readily available for the incorporated cells. Since vascularization is especially successful on long term, oxygenation can show interesting supportive qualities at bridging the period where the vascularized construct is not connected to the vasculature of the implant site yet, since it supplies the cells with oxygen on short term. [33; 34]

Oxygenation aims for the biomaterial to release oxygen gradually over the course of this time. These oxygen releasing biomaterials could prevent the necrotic core of a tissue due to low oxygen tension. Current approaches regard oxygen-carrying biomaterials (e.g. haemoglobin-based oxygen carriers) and oxygen-generating biomaterials (e.g. liquid peroxide). [35; 33; 36]

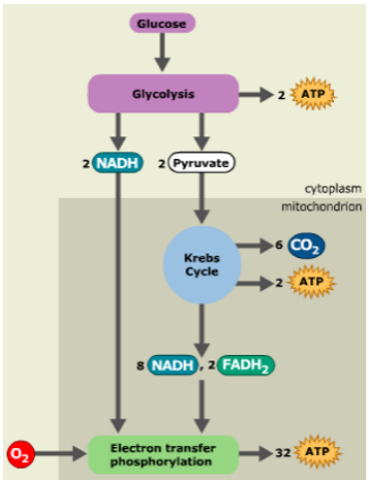

Figure 2: *Schematic overview of ATP generation in aerobic and anaerobic metabolic pathways*

As can be seen in figure 2, metabolic pathways operating with oxygen, result in a more efficient way of ATP production. However, oxygen alone can not keep these systems running, but multiple nutrients such as glucose are needed as input to generate these ATP molecules. In fact, it has been shown hMSCs can survive anoxia when supplied with glucose and the lack of glucose is the fatal factor in these anoxic regions. [37; 38; 39]

1.3 Metabolites

If oxygenation of a construct is successful, an important function of vasculature is overlooked; the supply of nutrients to cells. Nutrient deprivation of cells can result in autophagy, which has a pro-survival function. Autophagy is induced to stop the anabolic processes and allow cellular repair to keep cells viable and prevent further damage. Moreover, it increases the required level of stress needed for initiating cell death. When the damage is too large, apoptosis will occur to maintain tissue homeostasis. To prevent this from

happening, metabolic needs and their possible use within tissue engineered constructs are looked into. [40]

1.3.1 Metabolic needs of cells

Metabolic processes of the cell are widely studied, but they remain not fully understood. Metabolic processes consist of the intricate interplay between multiple metabolic pathways, regulated by intrinsic and extrinsic cell signals. Figure 3 shows an extremely simplified overview of the interactions of the main metabolic pathways. [41]

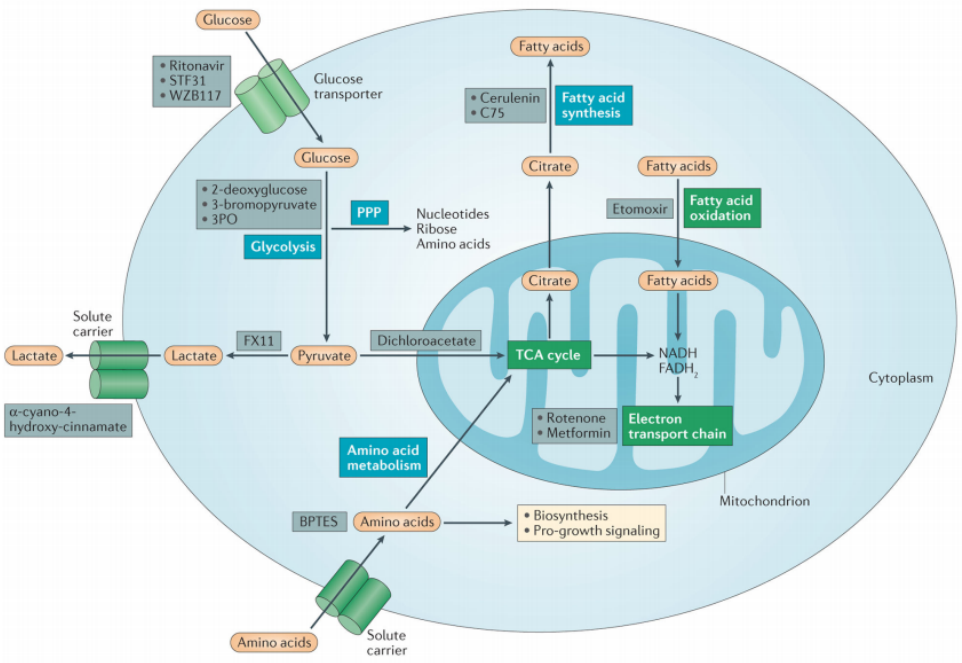

Figure 3: *Main metabolic pathways of mammalian cells, demonstrating their interaction. Figure adapted from O'Neill et al.[41]*

An important pathway is the glycolysis which yields, among others, pyruvate and 2 ATP molecules per molecule glucose, meaning it is a relatively inefficient way for generation of cellular ATP. Glycolysis is however beneficial for biosynthetic pathways via the conversion of NAD^+ to NADH and intermediates of ribose for nucleotides, amino acids, and fatty acids. [41] Moreover, no oxygen is needed for this pathway, explaining the important role it plays with hypoxic cells.

The presence or absence of oxygen is an important extrinsic signal for cells to induce a certain metabolic flux. In hypoxia, hypoxia-inducible factor-1α (HIF-1α) is activated, which is the main regulator of the (glucose) metabolic responses in hypoxic cells. It increases the expression of several target genes, such as those encoding for glycolytic enzymes and glucose transporters and it causes an increase in lactate secretion. Moreover, increasing evidence shows HIF-1α to be involved in regulating tissue regenerating properties and biosynthetic needs such as angiogenesis, cell survival and metabolism, to prevent cells from damage of hypoxic stress. Moreover HIF-2α, a similar transcription factor, is relatively unknown but is indicated to play a distinct role in glutamine metabolism for the promoting of metabolic switch in hypoxia.[42; 43]]

The tricarboxylic acid (TCA) cycle implements several intermediates from other pathways, such as

the glycolytic pathway. It is especially a major metabolic pathway in non-proliferative or quiescent cells (with exception of some stem cells) due to the highly efficient production of 36 ATP molecules in combination with oxidative phosphorylation. Since the TCA cycle operates within the mitochondria, it does requires oxygen to function completely. Two of the major products are NADH and $FADH_2$, which both are of importance to support oxidative phosphorylation. Moreover, several TCA intermediates are of importance for biosynthesis, such as amino acids and lipids.[44; 41]

Lastly the pentose phosphate pathway (PPP) serves key purposes regarding the support of cell proliferation and survival and is not fully dependent on oxygen, making it an interesting pathway for hypoxic cells. The PPP takes intermediates of the glycolytic pathway for the production of nucleotide and amino acid precursors, which is done via a non-oxidative branch. The oxidative branch of the PPP is responsible for keeping a favourable cellular redox environment, via the generation of reducing equivalents of NADPH.[26; 41]

1.3.2 Glucose

In a hypoxic environment, the glycolytic pathway is the main metabolic pathway activated for the production of ATP. The resulting pyruvate which normally goes into the TCA cycle as an intermediate, is converted into higher numbers of lactate. Due to the metabolic switch, an increase in glucose uptake is needed to reach the same levels of ATP. HIF-1α plays a large part by enhancing the glucose uptake of the cell and increasing the glycolytic enzyme activity. [41; 45]

To eventually be able to supply the right amount of glucose to cells in tissue engineered constructs, it has to be known how much glucose is needed. The aim of this thesis is to develop a system with which information can be gained on which metabolites are needed for hMSCs to survive anoxic conditions. Moreover it is of interest to obtain knowledge on the minimal concentration needed of these metabolites to result in optimal survival and functionality of hMSCs in these anoxic conditions.

Current gold standard in cell culture research is 2D, static cell culture. This consists of a monolayer cell culture, often in a cell culture flask, with medium which has to be manually refreshed. However, nutrient consumption by cells is continuous. In static culture systems, this leads to a continuous decrease of overall nutrient availability, while the level of waste products continuously increases.

1.4 Microfluidics

A way to tackle the limitations of static culture, is to implement a dynamic method. With a dynamic method, constant replenishment of the cell culture medium can be established. This allows for a constant nutrient grade and for waste levels to be as low as possible.

An often used dynamic method is microfluidics, which is a technology characterised by the engineered use of fluids at sub-millimetre scale.[46] PDMS is often used as a material for microfluidic chips due to its possibilities for implementation of robust structures, low level of auto fluorescence, and transparency. It has however some limiting aspects which have to be taken into account when working with PDMS, such as its hydrophobicity, porosity, and toxicity to cells when not fully cured. [47]

Within the microfluidic environment laminar flow, which is an important characteristic, has to be taken into account. Laminar flow allows for the parallel flow of two separate streams without mixing. The mixing of these fluids happens over time via diffusion or when they are forced to mix via the design of the channels. [48]

A big advantage of the use of microfluidics is the need for less materials and cells as opposed to the large volumes used in static cell culture. Moreover, the microfluidic environment allows for precisely measured, continuous exchange of media. Lastly, with the use of microfluidic devices, simultaneous manipulation and analysis, and precise control from single cell to tissues is possible. All in all, microfluidic devices allow for efficient, rapid automation of manual labour intensive tasks with minimal intervention.[47]

Another advantage of microfluidic systems is that they come in many forms and applications, the one used for this application are gradient generators.

1.4.1 Gradient Generators

The main goal of gradient generators, as the name already indicates, is to create a gradient of the fluids supplied to a cell culture or tissue. Gradients are biologically interesting for investigation of several processes such as tumor growth, disease development, and nerve growth guidance. Creating well-defined gradients can help study these phenomena in a controlled environment.[49; 50]

In gradient generators with separated cell chambers, cells with the same supply of nutrients will be grouped together, in contrast to a design with one big cell chamber over which a gradient is supplied. With this separation in cells, multiple conditions can be tested in parallel resulting in, for example, quick iteration toward a minimum of nutrient needs via functionality assays on chip

1.4.2 Aim

When combining all of the different aspects, the aim of this thesis is to optimise a dynamic set up which can be used to control nutrient supply for hMSCs in near-anoxia (0.1% O_2). The system will be optimised to run for a week, whilst creating a stable gradient over this period of time. A microfluidic gradient generator chip with separate cell chambers will be used so several nutrient concentrations will be able to be analysed parallel on chip. Moreover, different cell lines of hMSCs will be tested, with different coatings and culturing media to get an understanding of the biological processes which play a role in the success of this system. Preliminary data will be obtained via live/dead assays and a PrestoBlue assay.

1.4.3 Objectives

To achieve the aforementioned aims, the following objectives are formulated:

- Optimise the microfluidic chip
  - Determine the best design for the microfluidic chip
  - Determine the best flow rate for the dynamic system
  - Establish a stable gradient
- Optimise the dynamic system
  - Determine the optimum way to connect the chip to a syringe pump
- Get an understanding of the biological variables
  - Determine the best combination of hMSC-donor, coating, and culturing media

2 Materials

All chemicals used in the experiments are listed in the table on the following page, with their abbreviation, full name and use in the several experiments.

Abbreviation	**Full name**	**Manufacturer**	**More information**	**Use**
PBS	Phosphate-Buffered Saline	-	-	Used in multiple experiments
PDMS	Polydimethylsiloxane	Dow Corning	SYLGARD™ 184 Silicone Elastomer Kit	Production of microfluidic chips
FSS	Fluorescein sodium salt	Sigma-Aldrich	MW:412.3	Determining gradient of the chips
Tris	Trizma® base (Trometamol)	Sigma-Aldrich	MW:121.14	Preparation polydopamine coating
Dopamine-HCl	Dopamine hydrochloride	Sigma-Aldrich	MW:189.64	Preparation polydopamine coating
HCl	Hydrochloric acid	-	MW:36.458	Preparation polydopamine coating
NaOH	Sodium hydroxide	-	MW:40.00	Preparation polydopamine coating
COL	Collagen I	Corning	Rat Tail High Concentration 10.98 mg/mL	Preparation collagen coating
SFM	Serum-free medium	Sigma-Aldrich	D5030-10X1L	Preparation of serum free medium
NaHCO3	Sodium bicarbonate	Sigma-Aldrich	MW: 84.007	Preparation of serum free medium
Glucose	D-Glucose (dextrose)	Gibco	MW: 180.156	Addition to serum free medium
GOx	Glucose oxidase	Sigma-Aldrich	*kit*	Performing a glucose assay
HRP	Horseradish peroxidase	Sigma-Aldrich	*kit*	Performing a glucose assay
DAB	3,3' Diaminobenzidine	Abcam	*kit*	Performing a glucose assay
DMEM	Dulbecco's Modified Eagle Medium	Gibco	-	Culturing 3T3 cells
AMEM	Alpha Minimum Essential medium	Gibco	Nucleosides	Culturing hMSCs
FBS	Fetal bovine serum	-	Aliquoted by lab	Addition to cell culture medium
Pen/Strep	Penicillin-Streptomycin	-	Aliquoted by lab	Addition to cell culture medium
AsAP	ascorbic acid 2 phosphate	-	Aliquoted by lab	Addition to AMEM
-	GlutaMAX	Gibco	100X	Addition to AMEM
b-FGF	Basic fibroblast growth factor	-	Aliquoted by lab	Addition to AMEM
ITS	Insulin-Transferrin-Selenium	Gibco	100X	Addition to serum free medium
Live	calcein-AM	Sigma-Aldrich	17783-1MG	Viability assay
Dead	ethidium homodimer-1	Sigma-Aldrich	46043-1MG-F	Viability assay
D5	Draq5	Invitrogen	-	Viability assay
-	PrestoBlue	Invitrogen	-	Metabolic activity assay

3 Methods

3.1 Chip fabrication

Microfluidic chips were prepared using standard replication moulding. A 10:1 w/w mixture of PDMS and cross linking agent (Sylgard) was mixed and poured onto a negative mould, which has previously been prepared from a CAD model with standard soft lithography techniques. The wafer with the PDMS solution was set in a vacuum for 15 minutes at -0.08 MPa to remove all air from the solution. The wafer was placed in the oven at 65°C and cured over night. The PDMS was then peeled off the wafer and 1.5 mm holes were punched at the inlets and outlet to provide connection points for tubing. The PDMS and glass surfaces were plasma treated (Recipe 2, Cute, Femto Science, South Korea) and immediately after brought together to covalently bind the PDMS to the glass substrate to form the chip.

3.2 Polydopamine preparation

A Tris-HCl buffer was prepared with 10 mM Trizma and tuned with HCl and NaOH to a pH of 8.5. A 2 mg/mL solution of dopamine hydrochloride in the Tris-HCl buffer was prepared and used directly. This polydopamine (PD) solution was loaded into the outlet of the chip until it came out of the inlets and incubated at room temperature for 1 hour. After incubation the chips were washed three times with plenty mQ water, set to dry overnight at 65 °C and kept at room temperature until use.

3.3 Collagen preparation

A solution of 1% collagen I in PBS is prepared and kept at 4 °C until use. PD coated chips were coated with this collagen solution by loading it into the outlet, incubated at 37°C for 30 minutes and washed with PBS.

3.4 Preparation of serum free medium

For preparation of serum free medium (SFM), DMEM D5030 sigma powder without glucose and glutamine was used. 90% of the final volume of tissue culture grade H_2O at room temperature was measured out. 8.3 g/L powdered serum free media was added while gently stirring the water. 3.7 g/L $NaHCO_3$ was added, stirred until dissolved, and brought to final volume with tissue culture grade H_2O. The medium was sterilised by filtration using a membrane porosity of 0.2 μm and stored in the fridge until use.

3.5 Cell culturing

3.5.1 3T3s

3T3 cells (mouse embryonic fibroblasts) were cultured in high glucose DMEM (4.5 g/L) containing 10% FBS and 1% pen/strep in T175 cell culture flasks. The cell culture flasks were kept in an incubator at 37°C with 5% CO_2 and medium was refreshed every 3-4 days until the cells reached 80% confluency. These cells were used at a density of $2*10^6$ cells/mL to validate and optimise several aspects of the system.

3.5.2 hMSCs

Human mesenchymal stem cells (hMSCs) were cultured in aMEM containing 10% FBS, 1% pen/strep, 1% AsAP, and 1% glutamax, supplemented with 1 ng/mL FGF in T175 cell culture flasks. These cell culture flasks were kept in an incubator at 37°C with 5% CO_2 and medium was refreshed every 3-4 days until the cells reached 80% confluency. Only passage 1 through 6 were used in these experiments. A cell suspension of $2*10^6$ cells/mL in fully supplemented aMEM was prepared for use in the chip.

3.6 Assays

3.6.1 GOx assay

35μl of each sample was transferred to a BD falcon black 96 well plate. Next 40 U/mL horseradish peroxidase (HRP) and 400 U/mL Glucose oxidase (GOx) were combined 1:1 and 0,05% DAB assay (Abcam) was added, 35 μL of this assay solution was added to each well. Its absorbance was measured at 540 nm with a plate reader (infinite M200Pro, TECAN Trading AG, Switzerland).

3.6.2 Live/Dead assay

A live/dead stain was prepared with 0.5 μL calcein-AM and 2 μL ethidium homodimer-1 in 1 mL PBS. The samples analysed for live/dead were carefully aspirated and 0.5 mL live/dead stain was added and incubated for 15 minutes. Fluorescence pictures were taken with the EVOS fluorescence microscope (Thermo Fisher, USA) and analysed using ImageJ software.

3.6.3 Prestoblue assay

10% PrestoBlue reagent was directly added to each well and incubated for 90 minutes. Next, 100 μL of each well was transferred to a black 96 wells plate, which was done in triplo. Finally, the fluorescence was measured with a Victor X3 plate reader (Thermo fisher, USA).

4 Optimisation process

4.1 Static vs Dynamic culture

For quantification of the choice of a dynamic design over a static design, glucose measurements were taken over time in a static environment. 3T3s were seeded at 8000 cells/cm^2 in 0.5 mL serum free medium, enriched with 1 g/L glucose in a wells plate and incubated in near anoxia (0.1% O_2). Half of the conditions had their media refreshed daily and the other half twice a week. Samples were taken right before the media was replaced and analysed with a GOx assay.

The results of this experiment are shown in figure 4, in which a decrease in glucose level is observed at each time point as opposed to the glucose level of the medium, used for refreshment. Both the daily (figure 4A) and the biweekly (figure 4B) refreshment show a vast decrease in glucose levels. Moreover a wide variety is observed in these glucose measurements, which could be due to the entire volume being refreshed, possibly causing cells to be taken out of the wells resulting in a decrease in total glucose uptake.

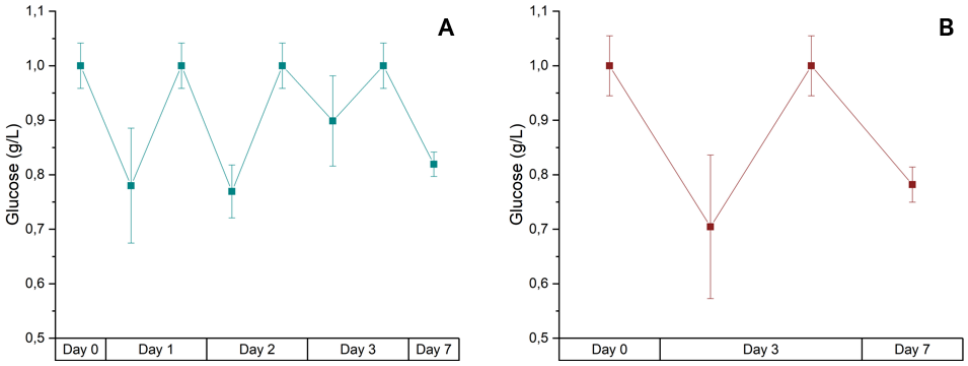

Figure 4: *Glucose levels in serum-free media at different time points with different refreshment rates. A) shows the condition with daily refreshments of medium, whereas B) shows biweekly refreshment of medium.*

To examine the effect of the total volume replacement, the same experiment was repeated. This time half of the conditions had half of the volume refreshed, the volume of the other conditions was fully refreshed. This experiment could show the effect of cells possibly being washed away during the previous experiment and if this would make a difference for the glucose uptake.

Results of this test are shown in figure 5, A shows the conditions where the entire volume was replaced and B the conditions where half of the volume was refreshed. Both conditions show a decrease in glucose uptake compared to figure 5, however even with the most optimistic approach, a vast and uneven decrease in glucose levels is observed in this static environment. With these large variations in glucose uptake it would be near impossible to narrow down to the minimal metabolic needs.

From these measurements, an estimation can be made on the glucose uptake rate by the cells in near anoxia. This calculation comes down to an uptake of glucose per cell of about 3.8 pg/min/cell. This is a gross estimation due to the vast day to day differences in glucose uptake and could have been measured more precisely with the use of the true number of cells, but supplies a grip for future calculations regarding cellular glucose uptake in near-anoxia.

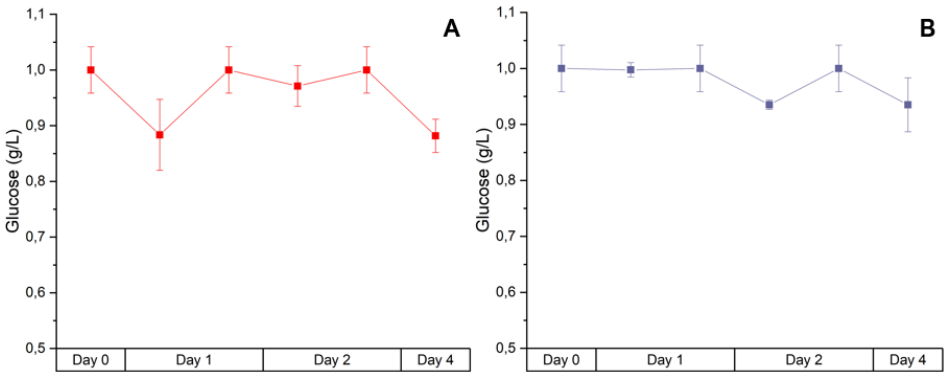

Figure 5: *Glucose levels in serum-free media at different time points with daily refreshment of medium with A) having its full volume changed and B) half of its volume*

A model, shown in figure 6, is constructed to show the theoretical values of glucose concentration at different starting concentrations and refreshment rates. A value close to 1.0 for In/Out ratio indicates no concentration gradient to occur within a chamber. This figure is constructed with data from *Deschepper et.al.* and *Moya et. al.*[37; 38] Figure 6B shows the in/out ratio on a zoomed-in scale, which suggests the lower glucose concentrations to mix the worst, if more concentrations would be added to this model.

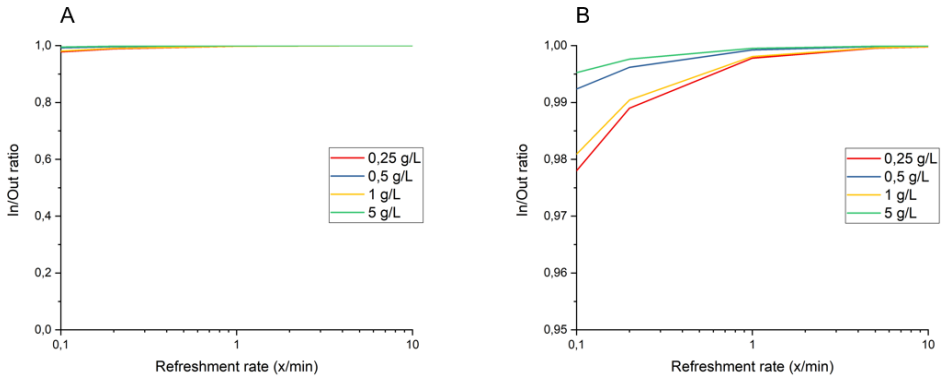

Figure 6: *Theoretical value for the ratio between glucose concentration entering the system and glucose concentration exiting the dynamic system, with different refreshment rates and starting glucose concentrations. B shows the same values on another y-axis*

This theoretical model with a refreshment rate of once per minute or faster would not result in a concentration difference, regardless of the starting concentration. Since the starting concentration will be changed throughout the experiment, it is of utmost importance to choose the right refreshment rate. Since a refreshment rate of once every minute is not feasible in a static culture, whereas dynamic systems can keep this level of available glucose steady, resulting in a reliable measurements for metabolic needs, confirming the choice of microfluidics over static culture for approaching this research aim.

4.2 Gradient generators

4.2.1 Requirements

Several requirements are set at the start of this project to make best use of the materials available and gain the most insight about the cell response on the exposed variables.

The first and arguably most important requirement is the generation of a stable gradient between the cell cultures. With a stable gradient, experiments can be conducted and conclusions drawn, based

on the additives and the relative function of these cells. Without this gradient, the cell chambers will be supplied with an unknown medium concentration and a concentration difference might occur between the chambers. This results in a varying level of nutrient supply for the cells in a chamber, as would be in a static culture and results in hard to interpret assays. To achieve a gradient, proper mixing between the two presented liquids is of utmost importance. As mentioned before, with microfluidics mixing occurs primarily via diffusion, due to the laminar flow at this small scale. This design has to give enough time for the liquids to diffuse before the next ramification and eventually before entering the cell chambers. This requirement is met via the use of a tree-like concentration gradient generator, going from two to eventually five concentrations. Moreover, by creating serpentine channels of sufficient length and amounts of turns via which the liquids are forced to mix, the mixing of the concentrations is optimised for a good gradient.

Furthermore, this project aim requires separate cell chambers in the chip. With such a design, cells with the same supply of nutrients will be grouped together, in contrast to a design with one big cell chamber over which a gradient is supplied. With this separation in cells, multiple conditions can be tested in parallel, resulting in a quick iteration toward a minimum of nutrient needs via functionality assays on chip. In addition, the separation of cells with different supply of nutrient concentrations prevents the cells from migrating towards the most favourable conditions. This is of importance since the cells are placed in harsh conditions, leading it to be difficult to find the minimal metabolic needs.

Moreover, the design should be of a low shear environment, due to the cells which will be combined in the chip. Shear has impact on hMSCs, a shear of 0.3 dyne/cm^2 or higher could result in differentiation, which is undesirable in this application since the effect on undifferentiated hMSCs is investigated. Moreover, differentiation can impact the cells' metabolism, which affects the data and eventually the application.[51; 52] For these reasons the design should allow for a flow resulting in a low shear environment, under 0.3 dyne/cm^2. On the other hand, the supply of nutrients and medium should be quick enough to prevent a concentration gradient over the cell chamber. This gradient could occur when the refreshment rate of the medium is too low, as is shown in figure 6 causing the cells at the end of the cell culture chamber to experience a lower level of nutrients than the cells at the beginning of the cell culture chamber. This could result in a behaviour difference within the cell culture, similar to the conditions in static culture, with living cells at the beginning of the cell culture chamber and dead cells at the end of the chamber after a week, which again results in an unreliable readout for the functionality assays.

With these requirements in mind, the designs were created in Solidworks (version 2019, DS) to use as a mask for the negative mold produced via standard soft lithography.[49]

4.2.2 Flow rates

In order to prevent concentration gradients to emerge within one cell culture chamber, the refresh rate of the nutrients has to be faster than the cellular uptake of those nutrients. Moreover, the resulting shear should be below 0.3 dyn/cm^2 to prevent any effect on the cells. The shear was calculated for different flow rates, using the following equation described by *Stone and Hollins* [53];

$$\tau = \frac{[2\mu u_{\max}]}{h} \tag{1}$$

Within this equation τ represents the shear stress in dyne/cm^2, μ is the fluid viscosity coefficient, u the flow rate, and h the height of the channel. Based on this calculation, the highest flow rate that should be used for the whole chip in this scenario is 50 μL/min, for the shear stress to stay just below

0.3 dyne/cm^2. The minimum boundary is set at a refreshment rate of the chambers for once every minute, figure 6 showed this to be fast enough to prevent a concentration gradient within a chamber. Since the chip has a volume of 8.25 μL, the minimal flow rate comes down to 8.25 μL/min/chip. With these measurements, the volume of the serpentine channels and outlet is neglected. This should not be a problem since there are no cells in this part of the chip, meaning the medium is not affected and still complete when entering the chambers. The minimal flow rate has to be higher than the rate of glucose uptake by the cells. With a flow rate of 8.25 μL/min/chip, a seeding density of 2*10^6, and a glucose saturation of 1 g/L, this comes down to a glucose availability of 5 ng/min/cell. As long as the glucose uptake per cell is lower than this value, no concentration gradient will occur along the cell culture chamber. It has been shown for the cells in static conditions in near anoxia to have a glucose uptake rate of 3.8 pg/min/cell, orders of magnitude lower than the glucose availability. This confirms a refreshment rate of once per minute will not result in a concentration gradient over the cell culture chamber.

It was chosen to test refresh rates of once, twice, and three times per minute, and the maximum flow rate calculated, respectively 8.25, 16.5, 24.75, and 50 μL/min. With this range it is expected to get a grasp on the ideal flow rate for the dynamic set up, one that does not affect the cells causing differentiation, but is also quick enough to not generate a concentration gradient within the chamber.

4.2.3 Designs

With the design requirements from section 4.2.1 in mind, several chip designs were established with several distinguishing variables. Each design facilitates for two incoming liquids and ends in five separate channels. Two adjacent serpentine channels will mix in the following channel, the average of both will be the resulting, new concentration gradient, causing a gradient to originate. When starting with two concentrations of 0% and 100%, and ending in 5 concentrations, final theoretical concentrations of 0%, 12.5%, 50%, 87.5%, and 100% will emerge.

The two variables were either long or short serpentine channels and two different shaped outlets. The outlets were either in a triangular shape, with straight channels from the outlet to the cell culture chamber, or rectangular with angular channels. The first will be referred to as the triangle outlet and the latter as the octopus shaped outlet. With these variables set, 3 designs were established which were tested. Two designs with long serpentine channels, of which one with a triangle outlet, the other with the octopus shaped outlet, and one design with short serpentine channels and the octopus outlet. The variables are clearly shown in figures 7 and 8. With these different designs the determining variables could be established as efficiently as possible and the best design could be chosen for this application.

As can be seen in figure 9, each of these designs consists of 5 oblong cell chambers of each 1,65 mm^2 in surface area and a height of 0.1 mm. The channels from the outlet to the cell chambers are 0.4 mm wide and the serpentine channels have a width of 0.1 mm. Moreover, all of the serpentine channels within a design are of the same length, the long serpentine channels with a total of 10 turns come down to a length of 10.75 mm each, the short ones, with 8 turns, 8.65 mm each.

It is hypothesised for the designs with triangle outlets to be the best, since the unevenly distributed turns on the octopus design might cause negative effects on the back pressure to occur. Moreover it is hypothesised for the designs with longer serpentine channels to perform the best. This is expected since the mixing mainly happens within the serpentine channels via diffusion, causing the need for an as long as possible distance to mix. Furthermore, mixing of the liquids is promoted in the turns, the more turns, the better the mixing will be. Taking all of this in consideration, the design with the triangle outlet and

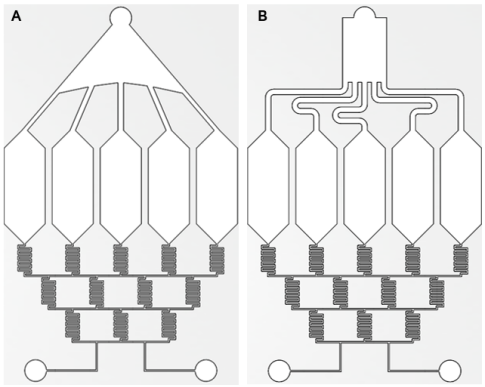

Figure 7: *Both outlet designs, A) shows the design with the triangle outlet and B) shows the design with the octopus shaped outlet*

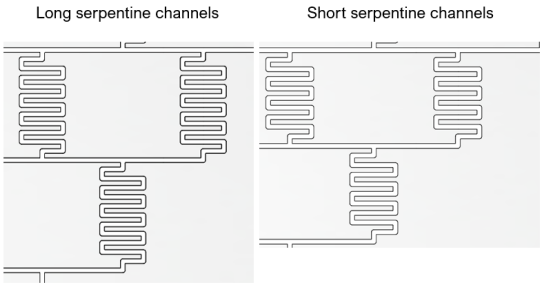

Figure 8: *Each long serpentine channel consist of a total of 10 turns, as opposed to the 8 turns of the short serpentine channel*

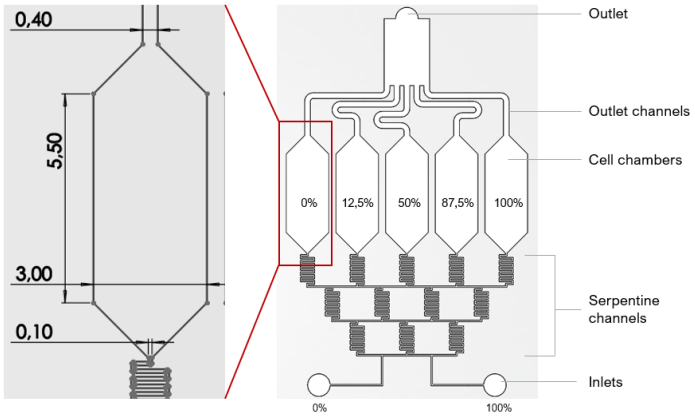

Figure 9: *Entire chip design with its expected gradients including each component and a close up of the most important measurements*

long serpentine channels is expected to be the best design.

4.3 Validation of design

The chip design is validated with the help of fluorescein sodium salt (FSS), since glucose is half the molecular weight of FSS, 180.156 and 376.27 respectively. Mixing happens via diffusion so if the FSS mixes properly, this will be the case for glucose as well, making it a valid choice for validation of mixing of the system.

The gradient was established by feeding one inlet with a solution of 1mM FSS in PBS, the other inlet with PBS. An inverted microscope (IX51, Olympus, Japan) with a DAPI filter (Omega XF02-2) fitted on the camera (ORCA-flash 4.0 LT, Hamamatsu Photonics, Germany) was used to measure the fluorescence in real time with 4X magnification.

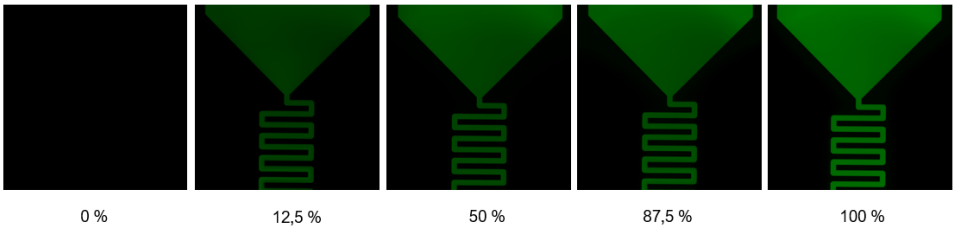

Figure 10: *Perfect fluorescence gradient of each chamber within a chip with their respective fluorescence value*

4.3.1 Results design validation

Pictures as seen in figure 10 were obtained and analysed by plotting the density profile using Fiji ImageJ software (Java, USA). From these profiles, all values above half maximum were averaged and normalised against the chamber with the highest average fluorescent value to find the percentage of the fluorescence intensity per chamber. From all three tested designs, the fluorescence measurements obtained were plotted against the theoretical fluorescence concentration, as can be seen in figure 11. In figure 11 the trend line is plotted from the theoretical value and the R^2 is calculated for each flow rate and design to quantify the mixing of the chip.

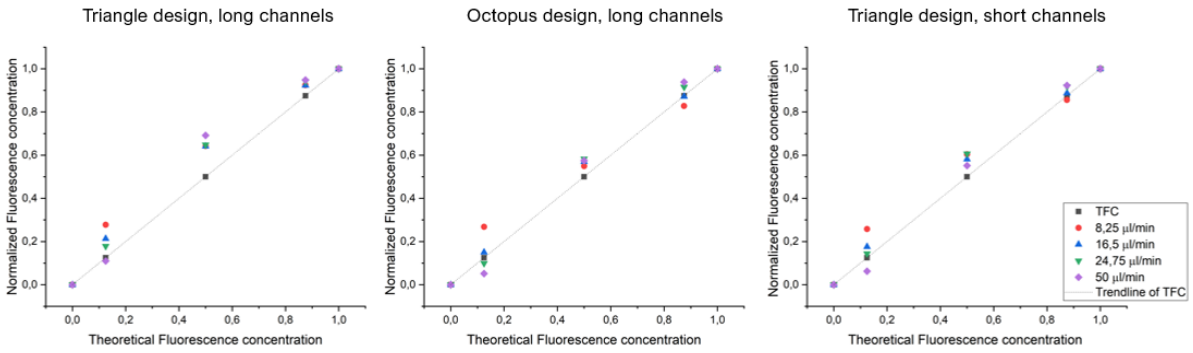

Figure 11: *Normalized fluorescence concentration per design at different flow rates plotted against the theoretical fluorescence concentration (TFC).*

Table 1 shows all obtained values of R^2 of each flow rate and design. In this table, the triangle design with the long serpentine channels shows the lowest values for R^2, indicating little agreement between the gradient generated and the theoretical gradient. Moreover, both the triangle designs do not perform very

		Chamber 1	Chamber 2	Chamber 3	Chamber 4	Chamber 5	R^2
Triangle long	**TFC**	1,000	0,875	0,500	0,125	0,000	1,000
	8.25 μL/min	1,000	0,924	0,643	0,277	0,000	0,972
	16.5 μL/min	1,000	0,923	0,641	0,214	0,000	0,9812
	24.75 μL/min	1,000	0,942	0,648	0,179	0,000	0,9816
	50 μL/min	1,000	0,948	0,692	0,110	0,000	0,9676
Octopus long	**TFC**	1,000	0,875	0,500	0,125	0,000	1,000
	8.25 μL/min	1,000	0,828	0,549	0,268	0,000	0,975
	16.5 μL/min	1,000	0,871	0,570	0,150	0,000	0,994
	24.75 μL/min	1,000	0,916	0,583	0,099	0,000	0,991
	50 μL/min	1,000	0,938	0,574	0,052	0,000	0,985
Triangle short	**TFC**	1,000	0,875	0,500	0,125	0,000	1,000
	8.25 μL/min	1,000	0,855	0,605	0,258	0,000	0,971
	16.5 μL/min	1,000	0,887	0,581	0,176	0,000	0,991
	24.75 μL/min	1,000	0,918	0,607	0,144	0,000	0,986
	50 μL/min	1,000	0,923	0,552	0,063	0,000	0,991

Table 1: *Normalized fluorescence concentration per chamber, per flow rate of the three designs, with the R^2 fitted to the trendline of the Theoretical fluorescence concentration (TFC).*

differently based on the values for R^2, but the short channels seem to result in better mixing in two of the flow rate conditions.

All of these values are still within a small range of one another and close to 1.0, resulting them to all have an acceptable gradient. The small differences in performance between the design with short and long serpentine channels might be explained by the fact that even the short design is near the optimum length for mixing, after which stagnation of mixing occurs. The triangle design with the short channels does however show an outlier with the fastest flow rate, this seems to be showing near perfect mixing which, due to the diffusion nature of mixing, seems highly improbable. This results in the disregarding of the short channels as a possible choice of design. It has been chosen to go forward with the octopus design with the long channels, due to its mixing to be slightly better than the other designs. Furthermore, this octopus outlet design allows for better control during the seeding of the chip, which is of importance due to the role the human factor plays during seeding.

Next, a remarkable observation is made in the flow rates in all three designs, the mixing improves with a lower flow rate, except for the slowest flow rate measured. Due to the linear nature of the diffusion, it was expected for the mixing to become better with a slower flow rate and eventually for the R^2 curve to flatten.[54]

A factor to keep in mind regarding the concentration gradient, is this dynamic system will have to run over a prolonged period of time, for which it has to remain stable. The current measurements have however taken place 15 minutes after the start of the flow, not being representative for the entire duration of the eventual experiments. Due to the volume needed for running an experiment for a week, and all R^2 values being within a reasonable range, it was chosen to evaluate the systems' stability with the lowest flow rate; 8.25 μl/min.

4.3.2 Gradient stability over time

The systems' gradient stability in the chip with an octopus shaped outlet and long serpentine channels was validated over time and checked at certain time points with fluorescence measurements. The results of these measurements can be found in figure 12 and table 2.

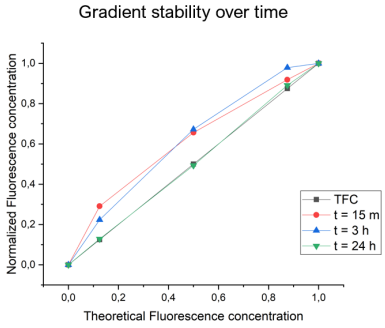

Figure 12: *Normalized fluorescence concentration of the design with an octopus shaped outlet and long serpentine channels with a flow rate of 8.25 µl/min over time plotted against the theoretical fluorescence.*

Time point	R^2
$t = 15$ m	0,946
$t = 3$ h	0,950
$t = 24$ h	1,000

Table 2: *R^2 of each set of normalized fluorescence values from figure 12*

When comparing the R^2 values from table 2, $t = 15$m and table 1, *'octopus long', 8.25 µl/min*, the value from table 2 is even lower, indicating worse initial generation of a gradient. However, both table 2 and figure 12 demonstrate an improving gradient over time.

The decrease in mixing with the lowest flow rate as observed in section 4.3.1 does not show through in the gradient in the long run. Its R^2 confirms this observation with the value at $t = 24$h to be 1, signifying perfect mixing, confirming the choice in design (octopus outlet with long serpentine channels) and flow rate (8.25 µl/min/chip). When continuing with an even lower flow rate than 8.25 µl/min/chip, the gradient stability over time will have to be assessed again.

4.4 Set up

4.4.1 Tubing

An important aspect of the dynamic system is allowing a flow through the chip. To achieve this, syringes are attached to a syringe pump and via tubing into a closed near anoxic environment, connected to the microfluidic device (figure 13).

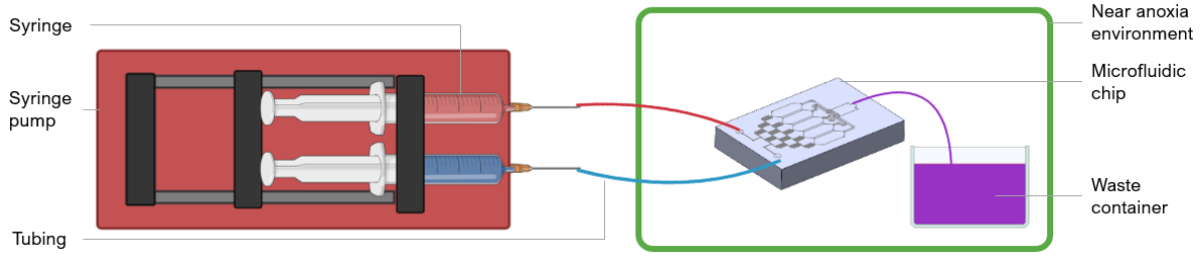

Figure 13: *Schematic overview of the microfluidic device attached to the set up*

The tubing is an important factor, since its length is approximately one meter, causing a lot of interaction between flow-through medium and tubing material. For this tubing several variables are considered, the needed length is fixed since this is determined by the lab space and dimensions of the Xvivo LAF-cabinet. The diameter, attachment method, and material are not fixed and can be optimised.

The diameter of the tubing is important for the back pressure, the smaller the inner diameter (ID), the higher the pressure to overcome by the syringe pump. The back pressure is dependent on the tube length as well, increasing with the increase of tube length. When the chip is seeded with cells, these

cells could result in a small increase in back pressure due to the narrowing of the channels, resulting in a possible shift in gradient. To make this pressure negligible, the back pressure could be increased mechanically. The combination of both a long tubing and a small inner diameter could however, result in the back pressure being too high for the application resulting in the desired gradient and flow rate over the cell chambers not being reached.

For this reason two inner diameters (0.01 and 0.02 inch) were tested for the tubing, it was chosen to keep the tubing the same over the entire chip, so the inlets would use the same type of tubing as the outlet would. To validate the choice of inner diameter, mixing was measured with FSS and plotted against the theoretical fluorescence concentration in figure 14, with its corresponding values for R^2 in table 3.

In figure 14 it is clear for the large inner diameter to result in a fluorescence concentration closer to the theoretical fluorescent concentration than the small inner diameter. This observation is confirmed with the calculated R^2 from table 3, since the value from the bigger inner diameter is closer to 1.0. It has been shown this mixing can improve over time, which can be the case with the small ID as well.

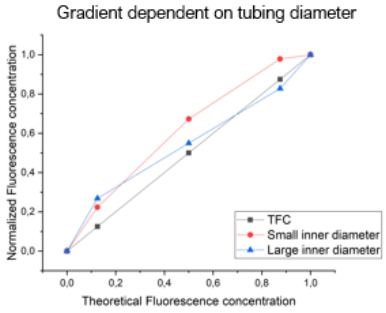

Figure 14: *Normalized fluorescence concentration of the chip with a small (0.01 inch) and large (0.02 inch) inner diameter of tubing and a flow rate of 8.25 µl/min over time plotted against the theoretical fluorescence.*

ID (inch)	ID (mm)	R^2
0.01	0.254	0,950
0.02	0.508	0,975

Table 3: *R^2 of each set of normalized fluorescence values.*

Another variable within the setup, is the attachment of the tubing into the chip. Several methods are described in literature; 1) irreversible attachment during production phase of the chip [55], 2) thin metal rods, inserted in both the tubing and the chip [56], and 3) direct insertion of the tubing into the chip, as per long standing practice [57].

To eliminate as many possible variables, it was chosen to directly attach the tubing into the inlets. Since the holes were punched with an 1.5 mm diameter and due to the plasticity of PDMS, the tubing can squeeze in tightly, creating a perfect fit for tubing with an outer diameter (OD) of 1.524 mm (0.060 inch).

When running the set up with this tubing, tearing of the inlets and outlets was observed as is shown in figure 15. Tearing is troublesome since it can cause leaking, which leads to uneven gradients, bubble formation, or even infection of the system.

A possible way to fix this tearing could be to seal and lubricate the connection point. When smearing Vaseline around the connection, it was expected to lubricate this connection point and prevent leakage as a result of torn PDMS, this however did not work and leakage was still observed.

Another similar way to fix the tearing, is to seal the connection point with super glue. This would stop the possible leaking when the inlets get torn. It could however affect the flow, when one inlet is torn but the other is intact, for this reason other options were considered to restore this issue.

The original choice of tubing (0.02 inch ID x 0.06 inch OD) was made from FEP (fluorinated ethylene-

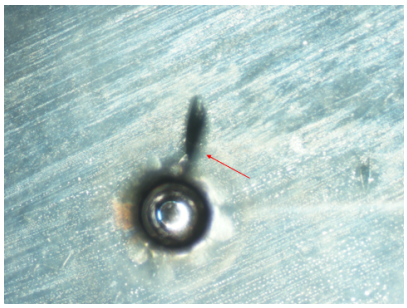

Figure 15: *Picture of an inlet with a tear, indicated with the red arrow, after operating the system.*

propylene) which is a very stiff material. A softer tubing was compared, for which a Tygon® Microbore tubing was chosen. An important aspect when choosing tubing is to consider their ability to not react with any of the elements of the flow-through medium. Some of the most important properties of FEP are it being chemically inert, UV resistant, and it does not absorb moisture from the air. The Tygon tubing is made from non-DEHP polymer material, which is specifically developed for medical device needs and highly biocompatible.[58] When running the same set up with this softer tubing, the inlets held up and no tearing was observed, indicting the stiffness of a tubing is a very important property for the application. This Tygon® Microbore tubing was used going on with these experiments.

4.4.2 Pulling vs Pushing

The direction the medium has to flow is fixed in the design, from the inlets to the outlets, but the side attached to the pump, is not. The pump however can either be used for pulling or pushing.

With pulling, the main benefit would be the unlimited amount of running time. The tubing connected to the inlets are inserted into a container of medium and the outlet is, via tubing and a needle, connected to a syringe on the pump. This syringe can easily be coupled off without creating bubbles in the chip, this way the syringe can be emptied during a run, increasing the possible running time. The difficulty with this method is creating the gradient, when the inlet tubings are not exactly the same length, a change might be observed in the gradient. Moreover, when the levels of medium are slightly differing due to one side causing more back pressure in the tubing, as well resulting in slightly differing gradient. Lastly, when trying the suction method, a bubble free chip could not be achieved, as can be seen in figure 16, confirming this method not suitable for this application.

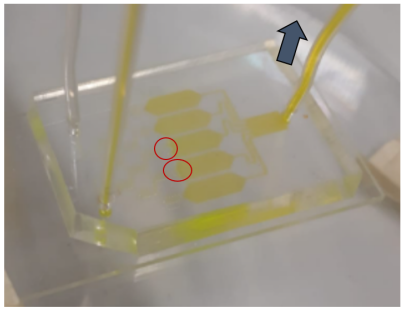

Figure 16: *Picture of a chip with created bubbles, indicated with red circles, after pulling the medium through. The arrow indicates the direction of flow*

With pushing, the inlets are connected to the syringes filled with medium and the outlet is connected via a tube to a waste container. The main limitation with this method is the volume of the syringes, this

volume together with the flow rate dictates the amount of running time for this experiment. To prolong the running time, the injected volume has to be increased, this could be done by changing an emptied syringe with a new one. Interchanging these, air is undeniably introduced in the system via the tubing, causing this to be the limiting factor. With this method, better control over the gradient in the chip is achieved, since both syringes pump with the same rate, creating equal force over the gradient generator. Since the syringe pump has its limitations with the use of syringes above the 50 ml, making this the limiting factor for the duration of the experiments.

Using 50 ml syringes with a flow rate of 8.25 µl/min over the chip, comes down to an running time of 8 days, when using 0.02 ID Tygon® tubing via the pushing method.

4.4.3 Bubbles

An often occurring and broadly studied problem within microfluidics are bubbles in the system. [59] Bubbles in the system would result in an uneven concentration gradient and flow through the chip due to obstruction. Moreover, when these bubbles get trapped in the cell chamber, the cells don't have access to the medium, causing increasing rates of cell death. Lastly the incorporation of bubbles could have an effect on the oxygen levels in the medium, again impacting the measurements.

To prevent bubbles from entering the system, the tubing has to be flushed thoroughly, after coupling each part of the set up. Moreover, during insertion of the tubing into the chip, care has to be taken so that no air gets trapped between the chip and tubing. This can be prevented by placing a droplet on the hole and making sure a hanging drop of medium is at the end of the tubing. Figure 17 gives a schematic view of proper connection of tubing and chip.

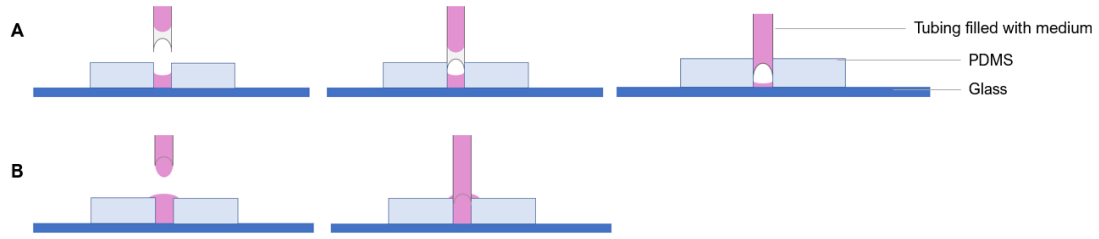

Figure 17: *Cross-sectional schematic view of tubing to chip attachment. A) Air bubble trapped in the chip after improper connection. B) Desired tubing-chip connection.*

If the tubing is attached bubble-free and no air is trapped in the serpentine channels, bubbles still can occur if they are introduced by the syringe or its connection system. It is of importance to prevent bubbles to be loaded into the syringe when filling it. To prevent this from happening, medium was degassed in the vacuum pump at -0.08 MPa for 45 minutes. After filling the syringes, they were tapped to release the bubbles from the side and pushed out. Moreover the syringes were swung to release the remaining bubbles to the top. These steps were sufficient for removing the gas out of the medium. The degassing step would be hard to use with an open container as with the pulling method. The high level of trapped gas in its medium could be the cause for the formed bubbles.

After tackling these different approaches to eliminate bubbles, they were still observed to form over time in the chip. One variable which has not been tested yet, was the filter. This filter was placed between the syringe and the needle to minimise the contamination risk when switching syringes and as an extra filtration step of the medium. This filter was wet before using, however small air bubbles were trapped within the filter, causing bubbles to escape over time to enter the chip. When the filter was taken out of

the dynamic set up, no more bubbles where observed, as can be seen in figures 18 and 19.

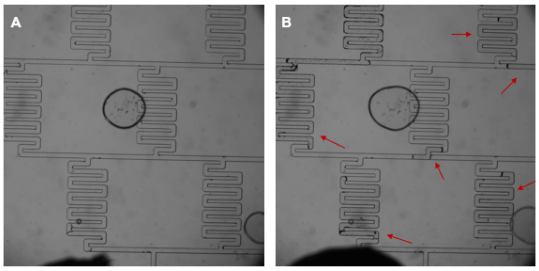

Figure 18: *Serpentine channels of a chip connected to the 0.2 µm syringe filter. Red arrows indicate bubbles in the system A) Directly after connection to the pump, B) After running the system for 15 minutes.*

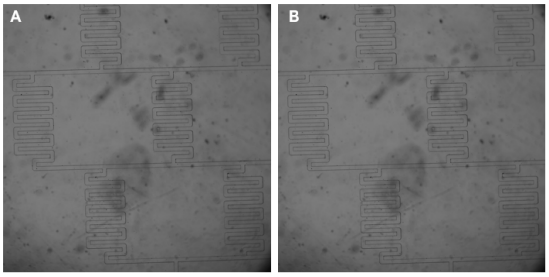

Figure 19: *Serpentine channels of a chip without the 0.2 µm syringe filter. A) Directly after connection to the pump, B) After running the system for 15 minutes.*

4.5 Coating

The chips are assembled from PDMS and glass as described in section 3.1. PDMS and glass are two inherently hydrophobic materials, causing cells to have trouble attaching in the chip. To overcome this hydrophobicity and increase cell attachment and survival, it is needed to coat the chip before cells are introduced to the system.

4.5.1 Polydopamine

Polydopamine (PD) is a relatively new chemical, since its first use in 2007 as a surface coating for inorganic and organic materials.[60] Since then it has been widely studied for its broad variety in applications in energy or water treatment, but most of all for its applications in the biomedical sciences. PD is especially interesting for its applications with biomedical microfluidic devices, where it helps turn hydrophobic surfaces permanently hydrophilic, or can assist chip bonding. Moreover it has several biofunctionalization characteristics, such as conjugating proteins, deposit metal, or even promote proliferation.[61] Due to most microfluidic devices being constructed with PDMS, the hydrophilic qualities of PD are especially appealing in this application. Moreover, it has shown for PD to increase the stability of MSC adhesion and multipotency, thus increasing the biocompatibility of PDMS-based microfluidic devices.[62] Figure 20 shows the polymerisation process and chemical structures of the polydopamine coating.

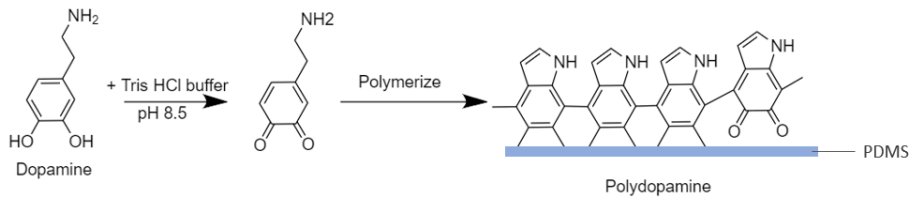

Figure 20: *Schematic presentation of the polymerisation of dopamine. Created using ChemDraw*

4.6 Seeding

4.6.1 Seeding methods

Initially, the chip design is made with the purpose of only the cell chambers and outlet being filled with cells. At the start of this project, a seeding method was optimised to seed just this upper half of the chip with a success rate of 75%.

After the coating was dried overnight in the oven at 65°C, the cell suspension was carefully loaded via the outlet with a p200 pipette (Eppendorf) up to the transition of the cell chamber to the serpentine channel, as can be seen in figure 21. A droplet of medium is placed on each of the inlets and outlet, and the chip was positioned in a petridish with a small container of PBS, closed with Parafilm to prevent evaporation and placed in an incubator with 20% O_2 and 5% CO_2. After these cells attached, they were washed with medium and stored in the incubator until used.

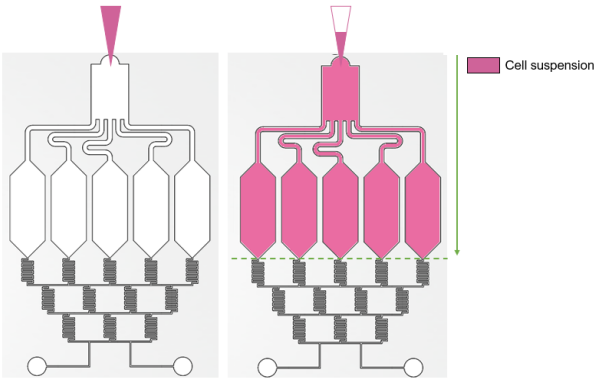

Figure 21: *Schematic representation of the first seeding method for the chips, where an empty chip is halfway seeded with a pipette*

Several problems were encountered with this seeding method; the first one being the formed bubbles in the cell chambers after cell attachment in the incubator. This was due to evaporation in the chip, through the PDMS, and can be prevented by covering the chip in its entirety with a tissue drenched with PDMS.

Moreover, with this seeding method, the serpentine channels were filled with air, which had to be pushed out by the medium in the washing step. Due to the small turns within those channels, air got trapped during the washing step. When manually pushing these bubbles out of the system, cells encounter an unknown quantity of stress, resulting in cell detachment and most likely cell death, causing the need for a new seeding method.

A method to prevent bubbles to form in the chip before attaching it to the system is to fill the chip in its entirety before loading the cells. With this method, a coated chip was loaded with PBS and formed bubbles are manually pushed out of the chip by simultaneously loading more PBS and manipulating the bubbles by pushing on them with a pipette tip. When the entire chip is bubble free, the cell suspension is carefully loaded via outlet until it comes out of the inlets, resulting in a fully seeded, bubble free chip. A schematic overview of this seeding method is shown in figure 22.

It was chosen to continue with these fully seeded chips due to the ease of seeding the chip bubble free via this method. Seeding the chip fully, instead of just the outlet and the cell chambers as its intention was, could have an effect on several aspects. The increase of cell count in the chip could cause a glucose gradient over the chip. If the glucose levels in the medium are low and the uptake rate of the cells is too

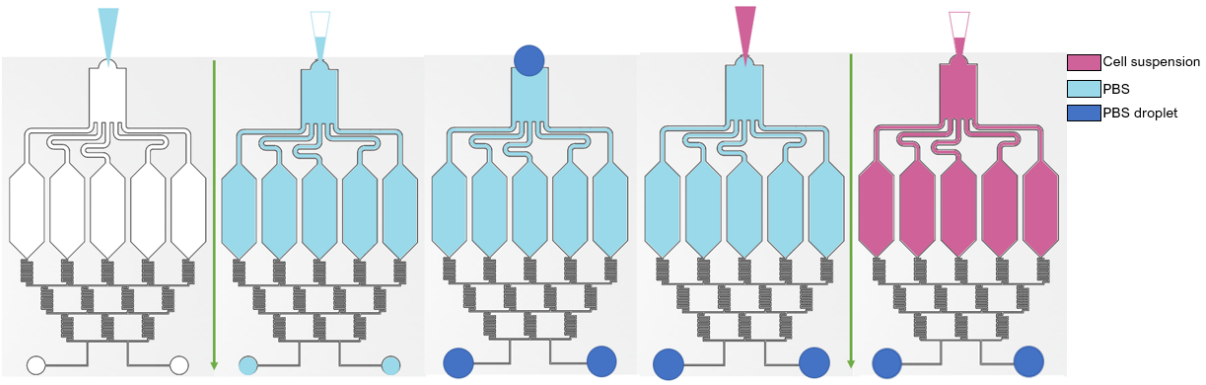

Figure 22: *Schematic representation of the optimised seeding method for the chips step by step, where a chip is first filled with PBS before being filled with a cell suspension*

high, the cells in the serpentine channels could affect the glucose levels in the medium to an extent where the true effect of the glucose levels on the cells in the chambers cannot be analysed.

Another variable that might be affected by the seeding is the gradient stability of the chip. Since the dimensions of this microfluidic system are at the sub millimetre scale, with the smallest features being 0.1 mm, an excessive increase in cell count could clog up the system. Since rounded hMSCs have a maximum diameter of 10 μm and attached cells are stretched over the surface, the height of these cells is just several μm, expecting to not have a significant influence on the gradient of the chip.[63]

4.6.2 Gradient stability with cells

To test the effect of cell seeding on the gradient stability, fluorescence is measured from two chips of which one is fully seeded, and the other one does not contain cells at all. The chips are attached to the syringe pump, with one syringe containing DMEM, the other 1mM FSS in DMEM. Photos are taken at different time points, analysed using Fiji ImageJ software (Java, USA)and the results are plotted against the theoretical fluorescence concentration in figure 23. The R^2 obtained from these data sets are shown in table 4.

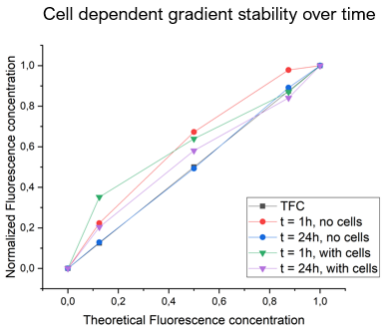

Figure 23: *Normalised fluorescence concentration of a chip with and without cells, measured with a flow rate of 8.25 µl/min over time plotted against the theoretical fluorescence.*

Time point	R^2
$t = 1$ h, no cells	0,950
$t = 24$ h, no cells	1,000
$t = 1$ h, with cells	0,929
$t = 24$ h, with cells	0,986

Table 4: *R^2 of each set of normalised fluorescence values.*

From figure 23 and table 4, it can be concluded both of the chips show an improvement of gradient over time. Although the values from the chip without cells does appear to have a slightly better gradient than the seeded chip, the R^2 of the seeded chip is still within an acceptable range. Moreover, it is possible

for the gradient of the seeded chip to still improve over time, but this is unfortunately not tested.

This data, together with the theoretical glucose uptake confirm this form of seeding of the chip to not have a negative effect on this dynamic system, thus approving this method of seeding.

The effect of this increase in cells on the glucose levels in the medium will have to be measured. If this does not show a significant difference as opposed to chips which are only seeded in the outlet and the cell chambers, this method could be used for obtaining preliminary data.

4.6.3 Glucose uptake

A glucose measurement is performed to see if the porosity of PDMS, the coating with PD, and fully seeding of the chip affect the glucose levels of the medium. Syringes were filled with SFM+1 g/L glucose, attached to the chip and samples were taken at several time points. The two conditions measured, were an uncoated and unseeded chip, and a PD-coated, fully seeded chip. A GOx assay was performed for determination of the glucose uptake by the chips and the results are plotted in figures 24 and 25.

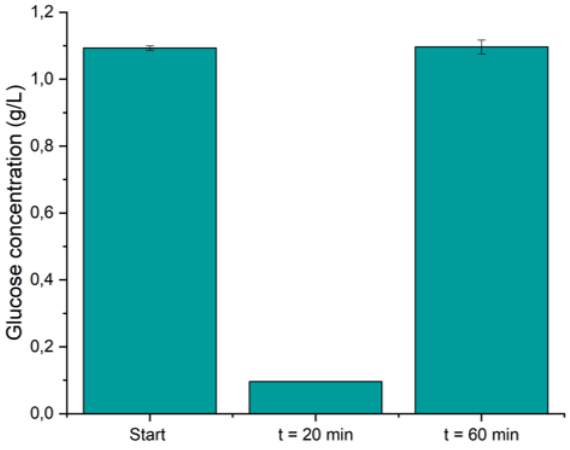

Figure 24: *Glucose uptake in a non-coated chip, without cells (n=2)*

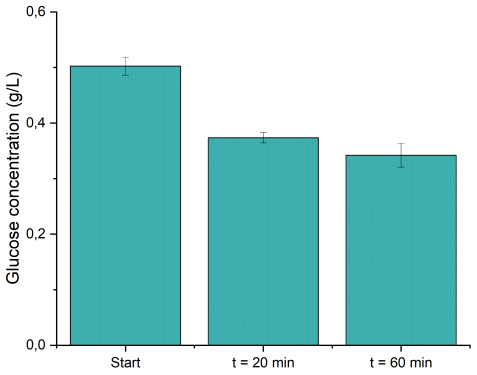

Figure 25: *Glucose uptake in a PD-coated chip, fully seeded with hMSCs*

Figure 24 shows the glucose levels in the output at $t = 0$, $t = 20$ min, and $t = 60$ min. The starting glucose level and glucose level at $t = 60$ min are similar, indicating no loss of glucose in the system. While the glucose level at $t = 20$ shows to be much lower, this could be due to not properly flushing through the chip, causing residual PBS from the system to be caught in the sample. Another possible explanation for this reduction in glucose output, could be the absorption of glucose by the system, becoming saturated before $t = 60$ min. If the second explanation is true, this absorption would most likely be due to the PDMS, since the other components of the setup do not have absorption qualities.

Figure 25 shows measurements of a PD-coated chip which is fully seeded with MSCs. The glucose levels are measured from the output at $t = 20$ min, $t = 60$ min, and from the starting liquid. In this graph a vast decrease in glucose levels is observed, which can be due to two reasons. The first reason could be a possible interaction between glucose and polydopamine, resulting in glucose to form a bond with the polydopamine resulting in a lower glucose concentration in the output. No evidence is found in literature about the possible interaction between glucose and polydopamine, only information is found on the interaction between PD and glucose oxidase. Another explanation for the observed decrease, is a glucose uptake of 10.68 pg/min/cell, which is vastly greater than the measured glucose uptake in static conditions from section 4.1, indicating a change in glucose uptake in hMSCs in near anoxia in static

versus dynamic culture, or a change in glucose uptake in hMSCs as a result of the cell-PD interaction. When this change in glucose uptake is due to the coating used, other coatings will have to be examined for their potential use in this system.

4.6.4 Collagen

Collagen is an intriguing material in the application for coating biomaterials. Collagen is a protein, of which several types exist in the human body, collagen type I is the most common type, abundant in the ECM and mainly known for its tensile strength.[64] Collagen I is currently successfully used as a coating material to improve biocompatibility or stem cell differentiation and can act as a cell adhesion protein for cells. [65] However, long term cell culture on a collagen coated surface is not optimal, due to cluster formation and cell sheet dissociation. The combination of collagen I with polydopamine counteracts these limitations and show an improvement of cell adhesion on PDMS. [62] Collagen is tested as a coating so it might counter act the increased glucose uptake, when this is indeed due to the polydopamine coating.

Glucose uptake

A GOx assay was performed to compare the glucose uptake in PD coated chips to the glucose uptake in COL coated chips. This was measured with fully seeded chips and a glucose concentration of 250 mg/L in SFM. 1 g/L glucose in SFM causes problems in measuring the fluorescence and the samples have to be diluted twice for readability of the plate. Each dilution creates an increasing error, and 250 mg/L has been shown to be plenty of glucose for hMSCs to survive in near anoxia, which is why it was decided to measure with 250 mg/L glucose.[37]

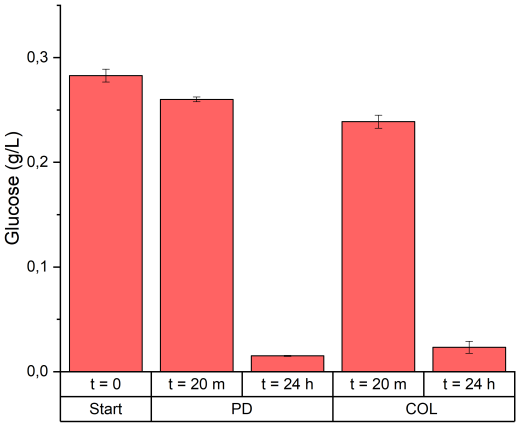

Figure 26: *Glucose uptake of PD-coated chips and COL-coated chips, both fully seeded with hMSCs*

Condition	Glucose uptake (pg/min/cell)
PD $t = 20$ m	11,4
PD $t = 24$ h	133,9
COL $t = 20$ m	22,0
COL $t = 24$ h	129,8

Table 5: *Glucose uptake per minute per cell at each condition shown in figure 26*

Results of these glucose measurements are shown in figure 26. With both chips a similar trend is shown of slight decrease in glucose levels after $t = 20$ min, of 0.02 g/L for PD and 0.04 g/L for COL, respectively a 8.0% and 15.6% decrease in glucose. This results in a glucose uptake of respectively 11.38 and 22.03 pg/min/cell. After $t = 24$ hours, the level of available glucose per minute as opposed to $t = 0$, dropped drastically in both chips, indicating a glucose uptake per cell of 133.87 and 129.75 pg/min/cell. Resulting in a respectively 94,6% and 91,7% decrease of available glucose in the medium. This contradicts

the theoretical model shown in figure 6, which states no concentration differences would occur when the refreshment rate is fast enough or the glucose concentration high enough, both of which was the case.

Table 5 shows the glucose uptake per cell per minute for each of the conditions. For $t = 20$ min, the glucose uptake does not differ much from the theoretical values found, 0.59-3.8 pg/min/cell. The glucose uptake at $t = 24$ hours does however show an incredible increase, which cannot yet be explained.

This decrease in glucose availability is lower than the comparative condition showed in figure 25, which shows a decrease of 0.13 g/L after 20 minutes. This difference between the values from figure 25 and 26 might be caused by the difference in starting glucose concentration.[37; 38]

Since both coatings do perform similarly, it was chosen to continue the experiments with PD-coated chips, since this coating takes less steps, allowing less chance of infecting the chip.

4.6.5 Final dynamic set up

Taken these variables into consideration results in the following setup; Two 50 ml syringes are connected to a 0.2 µm syringe filter (Acrodisc®, Pall corporation) and a 25g needle (BD Microlance). The needle is inserted into the Tygon® Microbore tubing with 0.02 inch ID, which is flushed with Biociadal ZF and PBS. The pump is started to flush through the tubing with plenty medium, after which the tubing is connected to the fully seeded and coated chip, flushed with medium and connected to a waste tube via the outlet tubing As is shown in figure 13 the dynamic system from the tubing until the waste tube is located in the Xvivo LAF cabinet with a temperature of 37.0°C.

4.7 Morphological changes

With the set up, coating, and seeding optimised, chips are prepared, seeded, and connected to the system in near anoxia. The chips are loaded with SFM on one inlet, and 1 g/L glucose in SFM in the other inlet and run over a week to obtain preliminary data on glucose needs. Pictures are taken daily with an eclipse TS100 microscope (Nikon, Japan) to assess the morphology, and at day 0 and 7 a live/dead assay is performed.

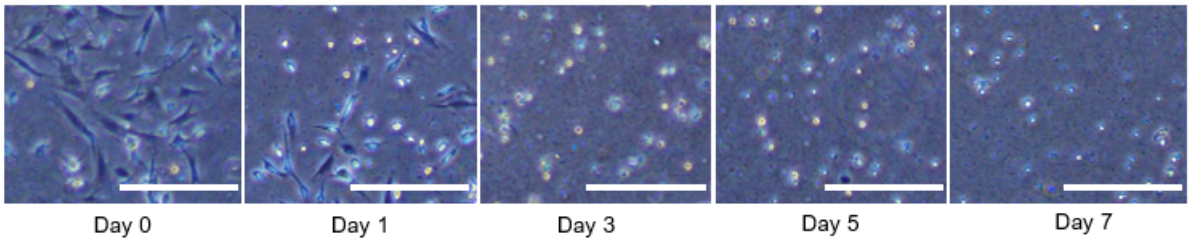

Figure 27: *Morphology of hMSCs in a PD-coated chip with 0.5 g/L glucose at day 0, 1, 3, 5, and 7, the scale bar represents 100 nm and live cells are indicated in green, dead cells with red.*

At day 1, morphological changes are already observed, as can be seen in figure 27, and from day 3 on, all of the cells seem to have a rounded phenotype as opposed to the elongated, stretched phenotype from day 0. The stretched phenotype implies proper attachment of the cell to the surface, the rounded cells indicate decreased attachment.

Cells placed in a harsh environment have a backup-system causing them to survive these conditions. One of these processes is autophagy, it increases the threshold of stress the cell can withstand before the induction of cell death. When cell death is induced, components are released into the micro environment,

which can serve as nutrients for the surrounding cells. This results the true effects of the conditions to be noticeable from 48 to 72 hours.[40; 66] This explains day 3 as a critical time point for observations of changes in morphology. Before this time observations are not representative of the true behaviour of a cell on a certain condition.

These changes are shown in all of the glucose concentrations, whereas at least the cells in the condition with 1 g/L glucose are supposed to stay fully attached.[37] Since this method was shown to work with 3T3s, few variables could be the cause of this change in morphology, either the flow rate or the choice of donor.

Moreover, the live/dead assay from figure28 indicate most of these cells to be alive, but does not say anything about the state these cells are in, indicating the cells to possibly be in a quiescent state.

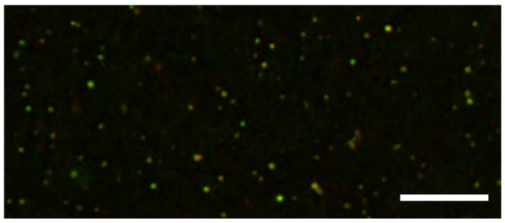

Figure 28: *Live/Dead assay at day 7 of dynamic culture of hMSCs in near anoxia with 0.5 g/L glucose*

4.7.1 Flow rate as a determining factor

To test if the flow rate is the determining factor, hMSCs were seeded at 7600 cells/cm^2, with 0.5 mL/well in a 24 wells plate, with either 0 g/L or 1 g/L glucose in SFM in near anoxia. Pictures were taken daily with an eclipse TS100 microscope (Nikon, Japan) and shown in figure 29

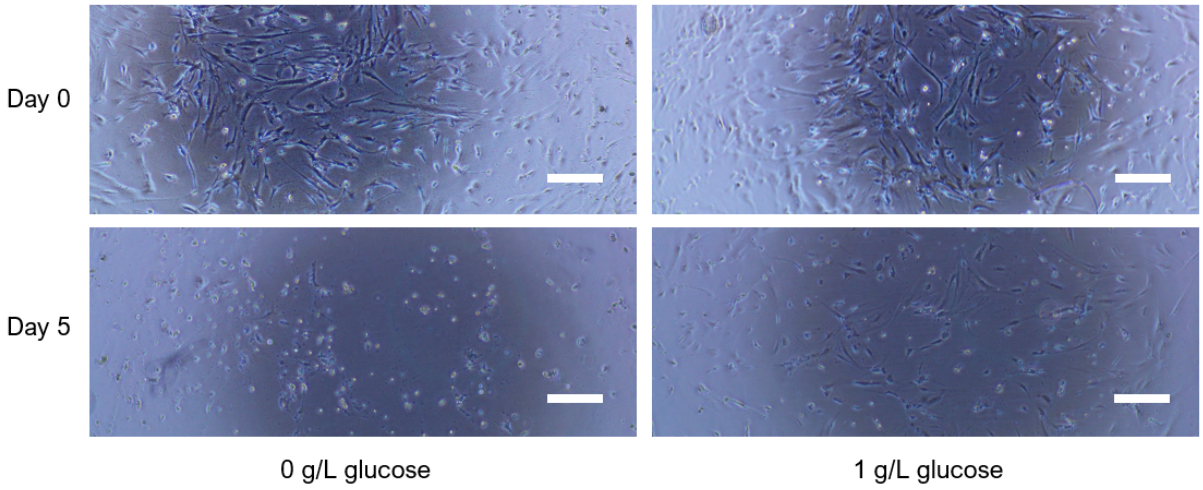

Figure 29: *Morphology of hMSCs in at day 0 and day 5, the scale bar represents 100 nm*

The cells in both 0 g/L and 1 g/L glucose express a more rounded phenotype in day 5 as opposed to day 0. Day 5 in static culture compared to dynamic culture has a lower level of rounded cells, suggesting a small part of the morphology changes could indeed be due to the flow rate and the shear stress accompanying this flow. Many cells do however still show a change in morphology, indicating this to be due to the choice of hMSC-donor.

4.7.2 Quiescence

A quiescent cell would show to be viable, but not metabolically active, which is why a PrestoBlue assay is performed on these cells, of which the results can be found in figure 30. A PrestoBlue assay contains the functional substance resazurin, which is converted into the fluorescent resorufin in metabolically active cells.

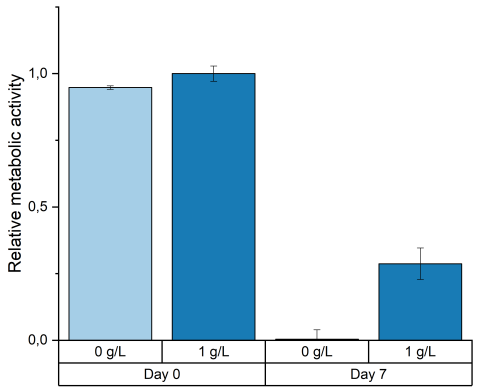

Figure 30: *Metabolic activity over time of hMSCs in static culture with either 0 g/L or 1 g/L glucose in SFM*

From figure 30 it can be observed for the metabolic activity for cells without glucose to be close to zero, which would be expected if the cells have died, the live/dead assay of 1 g/L however, showed a large amount of viable cells, indicating a quiescent state for these cells. The condition with glucose shows a decrease in metabolic activity of approximately 75%, this condition however shows cells of both phenotypes, suggesting the metabolic activity to be a result of the cells which are not rolled up.

From this it can be concluded the rounded cells are indeed cells in a quiescent state, next to their lack of metabolic activity, it is to be expected for cells which are not attached, to flow out of the chip in the dynamic system. For these reasons a combination of variables will have to be tested with as goal to keep the cells attached over time in anoxia. These variables are coating of the chip, choice of hMSC-donor, and medium used in the chip.

4.7.3 Determining factors

Coating plays a large part in cell-material adhesion, making it this is an important variable to optimise. To find the optimal coating, its effect on cell behaviour was observed. PD coated cover slips are compared to PD+COL coated cover slips, and to a non-treated wells plate as a control.

As mentioned previously, another possibility for the observed morphological changes, is a poor hMSC donor. The supply of stem cells depends on the local hospital, which supplies a wide variety in quality of hMSC donors. To test if the right donor was chosen to use for these measurements, three donors were tested on their metabolic activity in near-anoxia and normoxia. These donors are referred to with their given numbers: D72, D86, and D302.

Lastly, various medium are tested; aMEM, SFM, and SFM supplemented with ITS. The reason to use SFM instead of cell culturing medium, such as aMEM, is for the eventual possible applications within tissue engineering, due to the lack of serum.[67] This lack however might result in these stem cells becoming apoptotic. An artificial replacement for FBS, the serum generally used in cell culturing medium,

is Insulin-Transferrin-Selenium (ITS). Insulin is a naturally occurring hormone, increasing glucose uptake of the cell, transferrin is a transport protein mediating iron transport and helps reduce toxic levels of radicals, and selenium is used to stabilise the oxidative metabolism of the cell.[68; 69; 70] With the addition of selenium, the metabolic flux will entirely be caused by oxygen depletion of the environment. In this experiment, the standard supplemented aMEM was compared to SFM+1 g/L glucose and SFM+ITS+1 g/L glucose, where aMEM acts as positive control.

4.7.4 Optimisation of biological variables

To find the best condition, all of the conditions of each variables are combined with one another and tested both in normoxia (21% O_2) as well in near-anoxia (0.1% O_2). These conditions are tested in static culture with daily refreshment of medium, in section 4.1 it has been shown it is not a perfect representation, but insight in the best functioning combination regarding optimising the biological variables will be gained. For analysis of the cells' morphology, pictures were taken daily using the EVOS fluorescence microscope (Thermo Fisher, USA). Moreover a live/dead stain was done at day 0 and day 7, as well as a PrestoBlue assay for determining the metabolic activity.

LiveDead assay

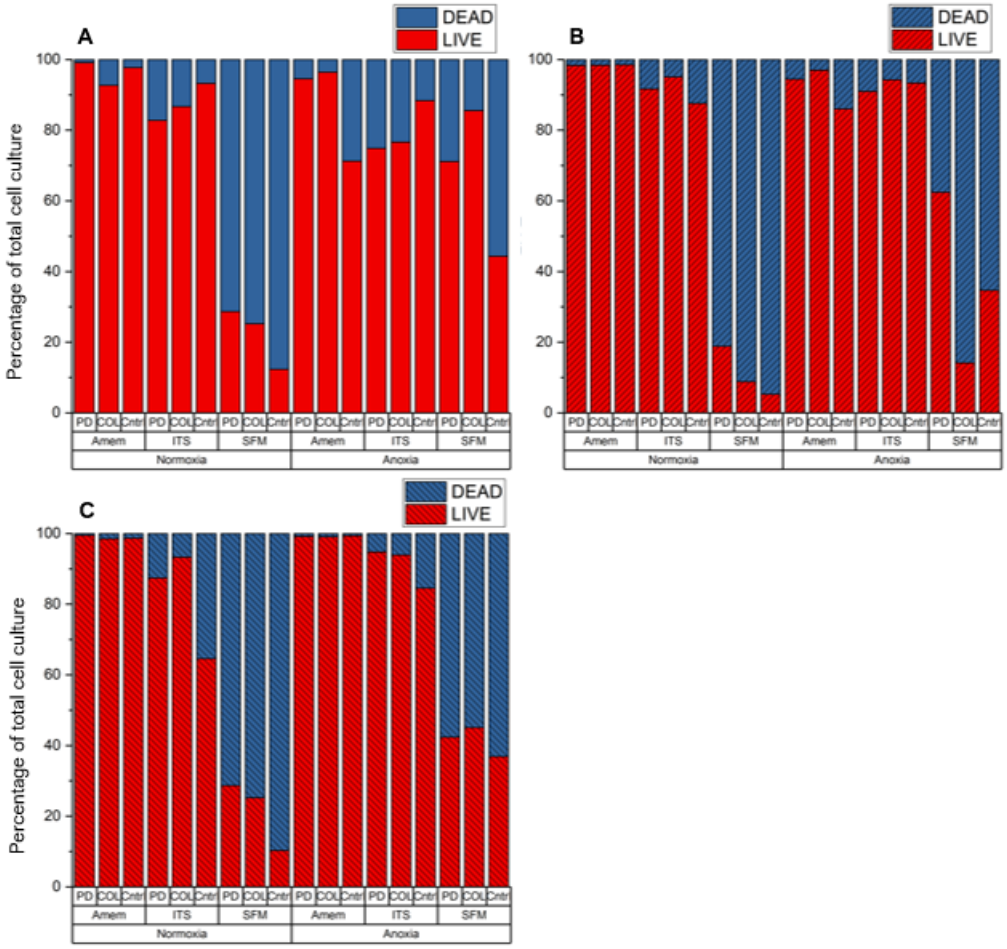

Figure 31: *Percentages of live and dead cells in each condition, of A) Donor 302, B) Donor 72, C) Donor 86*

The graphs in figure 31 show the percentages of live and dead cells of the population of each condition.

With donors D72 and D86, a significant share of the cells in serum free media are dead cells. With donor D302 in normoxia it shows the same trend, anoxia however shows very different results for both ITS and SFM, suggesting D302 to have a different reaction to SFM as opposed to D72 and D86. From the graphs of D72 and D86 it could be concluded the enrichment of SFM with ITS to have a drastically positive effect on cell viability. This result is in line with the expectations, and is quite promising for the continuation of this project.

These graphs are however not representative for what is actually happening, due to the way this assay was performed. Even though the media was aspirated carefully, it is not fully preventable to not take up any cells. If cells were to be aspirated from the wells, it is most likely for it to be the dead cells, due to their lack of attachment properties to the surface, which is why the actual cell count is of interest. The cell count is all normalised to day 0.

Cell count

With the relative cell count shown in figure 32, drastic increases and decreases compared to day 0 are observed. In all cases, aMEM results to the greatest increase in cell count, this was to be expected since aMEM is tuned to the needs of hMSCs. Within this group a vast difference arises as to which coating performs the best, with D72 and D86 in anoxia, a coating of PD results in less proliferation and COL and control are quite similar. With D302 in anoxia, the control is actually vastly lower than PD and COL. There is however no continuing trend observed for the coatings in normoxia so no conclusion can be made for this part.

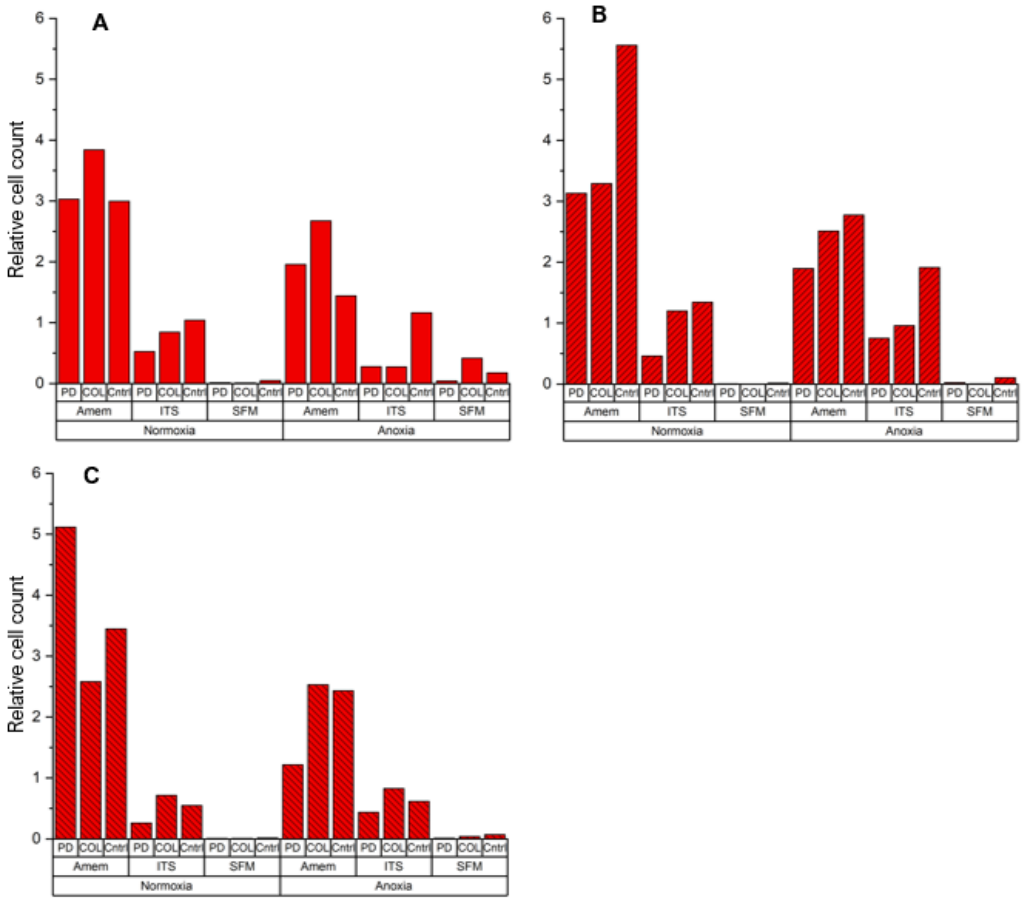

Figure 32: *Relative increase in cell count of live and dead cells in each condition, of A) Donor 302, B) Donor 72, C) Donor 86*

Another observation is the vast decrease in cell count for the SFM-conditions. All of the values for these conditions are below 1, indicating a decrease in cell count compared to day 0. With D72, D86, and the normoxic conditions of D302 these values are even very close to zero, where the anoxic conditions of D302, especially the COL-coated one, still show some degree of cell viability. Cell survival in anoxic conditions, while the normoxic counterpart shows no survival is striking, since an anoxic environment is more harsh and is thus to be expected to always show less cell viability when compared to the normoxic condition. The overall decrease in cell viability with SFM can be explained by the need of serum for survival. When looking at the ITS conditions, they are around (for D72 and D302) or just below 1 (for D86 and anoxic D302), indicating no big changes in cell count compared to day 0. All of the donors show COL to achieve better than PD in both normoxia and near anoxia. Moreover the control surface seems to be best for proliferation, only with D86 it is similar or slightly worse than COL.

From a proliferation point of view this would result in choosing ITS enriched SFM over plain SFM and a coating of COL for further use, since aMEM and the no-coating are only for control purposes. Moreover D72 shows more proliferation than D86, making it a more desirable donor. Proliferation is not necessary, but the most important factor is not to have a great decrease in cell numbers. Moreover, proliferation might indicate proper cell function, making it a quick variable for determining the right conditions. D302 shows contrasting results when compared to both D72 and D86, which is why this one is dropped as an option.

Proliferation is not the only factor determining how well cells perform under these conditions. Since the eventual application regards the cells metabolic needs, the metabolic activity of the cells can supply us with a clear distinction of the best condition.

Metabolic activity

The graphs in figure 33 show the relative metabolic activity of each condition, normalised to day 0. The first observation is the overall increase in metabolic activity when compared to day 0, only one condition is slightly under 1, with a value of 0.95, indicating an overall increase in metabolic activity. The extent to which the activity increased does vary between the donors, where the maximum relative metabolic activity for D302 is about 12, D72 and D86 go up to 22 and 30 respectively. This difference of metabolic activity between the donors is to be expected, since every donor has a distinct and slightly varying functionality and metabolism. In literature, the donor dependency on activity is widely discussed, and a bigger difference between the donors is shown with the metabolic activity, than with a viability assay.[71]

Although great differences are shown in these graphs between the donors, a some trends can be distinguished. The first being that in all cases, an increase is observed in anoxic conditions compared to the normoxic conditions. This increase can be explained when looking at the difference in aerobic and anaerobic metabolic pathways. To achieve the same amount of ATP, the influx of glucose by the cell has to be vastly greater. This could lead to the cells in anoxia to be more active as to recruit glucose for the cell to take up.

Moreover, the cells in SFM express by far the greatest increase in metabolic activity. In normoxia for all donors the increase with aMEM is higher than the increase with ITS. The latter can be explained by the fact that aMEM is supplied with everything the hMSCs need to proliferate and survive, and the ITS conditions only are supplied with the bare minimum, supplemented with serum to help increase survival rates via an increase in glucose uptake and reduction of toxic radicals. However, this does not explain the drastic increase in metabolic activity with the SFM conditions. When hypothesising the outcome,

it was expected for this condition to be the lowest of all since it is as well the harshest condition. The metabolic activity of a cell which is nearly dying is expected to be incredibly low due to the lack of ATP production, moreover it was shown in figure 32 this condition hat the lowest number of cells.

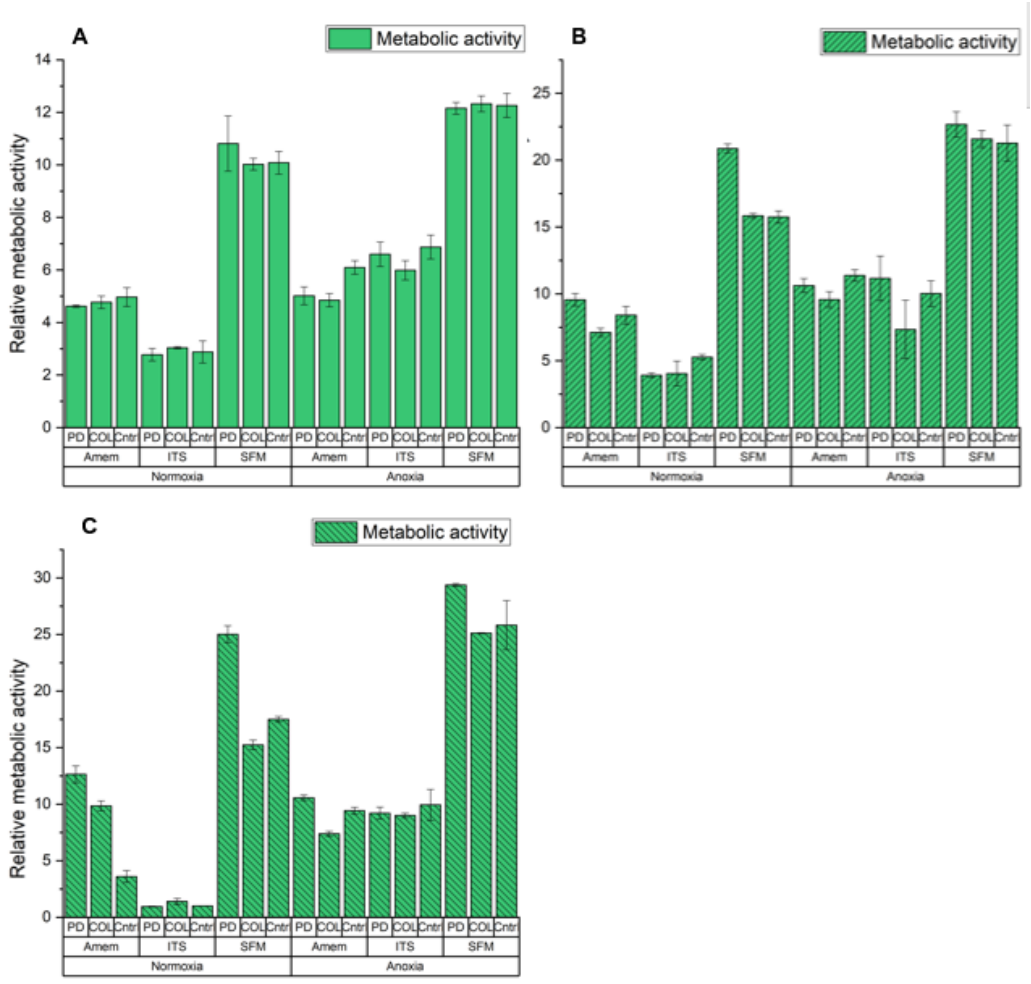

Figure 33: *Relative metabolic activity in each condition, of A) Donor 302, B) Donor 72, C) Donor 86*

In anoxia the relative activity of cells in aMEM and ITS vary between donors, but are overall quite similar, with a value of around 10 for both D72 and D86, but much higher for D302. This is quite promising for the continuation of the this project, since it would mean the addition of ITS to SFM to be sufficient to support the hMSCs, acting closely like aMEM without having to supplement the medium with more variables.

Regarding the effect coating has on the relative metabolic activity, only a few assumptions can be made. Only in SFM, cells on PD-coated surfaces seem to result in an increase in metabolic activity. Moreover, COL-coated surfaces seem to perform less other surfaces in anoxia. The final observation regards the value for the control surface with aMEM in normoxia for D86, this value is vastly lower than the other surfaces with the same conditions, this would mean both of the coatings increase the metabolic activity, this can however not be confirmed with other data from these graphs.

Metabolic activity and cell count

In figure 34 the relative cell count and relative metabolic activity are layered to provide an compre-

hensive overview of the interaction between the outcome of both assays. With all of the conditions, the cell count is, in a descending order; aMEM, ITS, and SFM. This suggests the same trend to occur for the metabolic activity since metabolic activity is to quite some extent dependent on the cell count. An overall trend can be found which is partly contradictory to the hypothesis, a decrease in relative metabolic activity can be observed from aMEM to ITS, as expected, SFM however exceeds all values for metabolic activity, while the cell count of SFM-conditions is decreased by a great deal. This observation suggests the readout of the PrestoBlue assay to not solely be dependent on the true metabolic activity of the cell, but it might react in some way with dead cells or the medium supplied. When the vast increase in PrestoBlue fluorescence is due to the medium, this would either have to show in the SFM+ITS-conditions, or the addition of ITS would have to counteract these fluorescence inducing aspects.

Literature shows indications of resazurin reduction to resorufin (the active substance from PrestoBlue) to take place intracellularly, more specifically it is suggested to take place in the mitochondria.[72; 73] The role of the mitochondria within metabolism is to enable oxidative metabolism, which goes hand in hand with an elevated metabolic activity of the cell. HIF-2αhas been shown to induce several processes in the mitochondria, possibly causing an increase in resorufin formation.[43] However, the only difference between SFM and SFM+ITS is the addition of serum, whatever causes the vast increase in fluorescence signal should thus be counteracted with the addition of serum, or the cell debris caused by the drastic cell death should have some effect on the fluorescence.

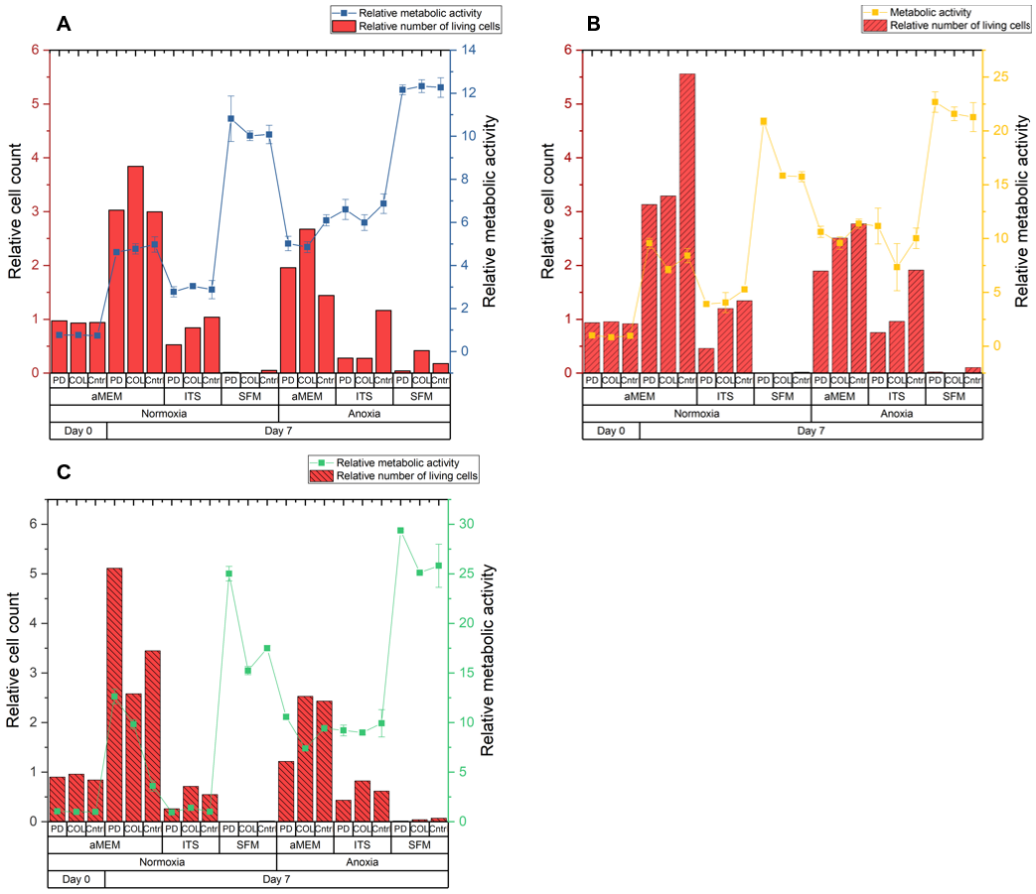

Figure 34: *Combined graphs of relative cell count and metabolic activity in each condition, of A) Donor 302, B) Donor 72, C) Donor 86*

Moreover, it has been shown for cyclodextrins to interfere with resazurin-based cell viability assays.

This is done via either the inhibition of the uptake of resazurin, or via the enhancement of the fluorescence signal of resorufin.[74] From current data no conclusions can be drawn as to why these extreme values for metabolic activity are observed.

Metabolic activity per cell

When plotting the metabolic activity per cell, An interesting observation is the increase of metabolic activity per cell in cultures in SFM+ITS compared to cultures in aMEM. Moreover, in all cases PD-coated surfaces seem to improve these values the most. The same conclusion can be made, since the metabolic activity per cell for cultures in SFM are sky-rocketing compared to the other media. It was however already concluded for the SFM to be not the best choice for this purpose, so when putting SFM to the side, more observations can be made.

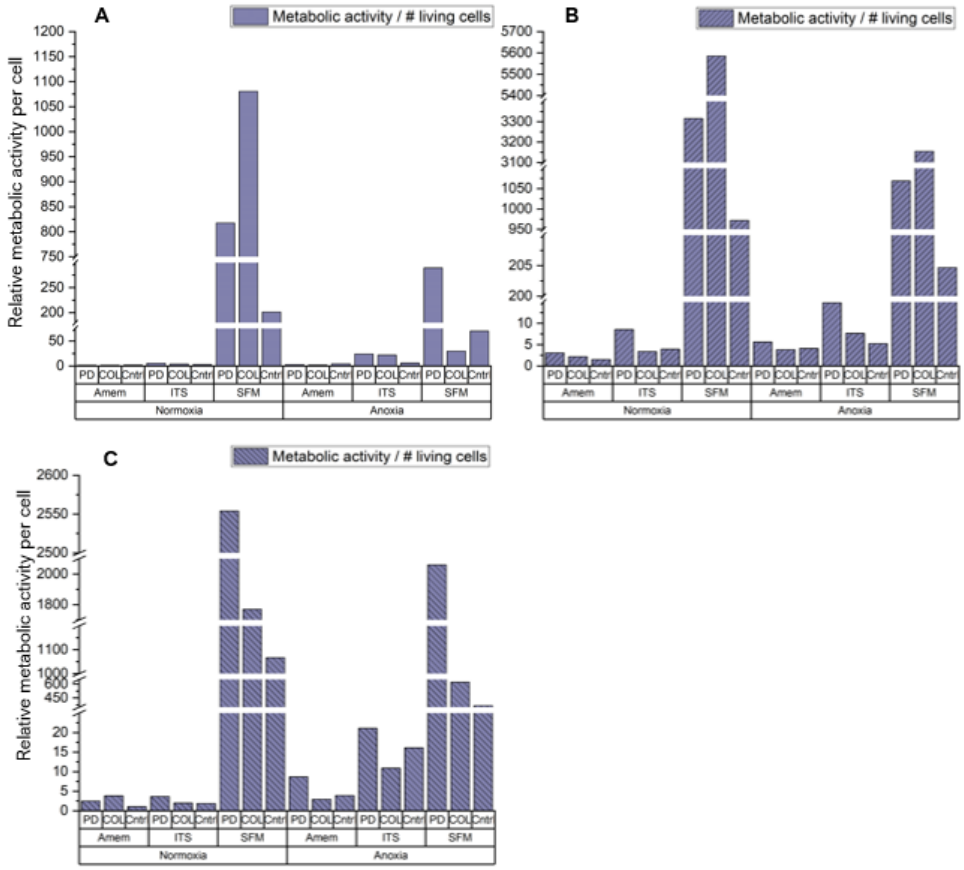

Figure 35: *Relative metabolic activity per cell in each condition, of A) Donor 302, B) Donor 72, C) Donor 86*

The main outstanding of all results is the extreme values of metabolic activity of cells in SFM, both in normoxia as in anoxia. When trying to explain these results, it is helpful to have a look at the chemical reaction of the non fluorescent resazurin to the highly fluorescent resorufin, as is shown in figure 36. Two possible explanations have been given thus far; the temperature might have an effect on the functionality of the SFM or a component acts in a similar way as the methylated cyclodextrins. With both of these explanations it has to be kept in mind the effect was apparently (partially) counteracted with the addition of ITS.

Moreover, conventional culturing medium such as dMEM and aMEM enriched with their corresponding additives usually has an expiration date of 30 days due to contamination risk. However, due to

expiration dates of each individual supplement, it is often not used for longer than 3 weeks. Since SFM is prepared ourselves and information on its shelf life is limited, it would be of use to determine its functionality at several time points. It might even be the case for some supplements to become unstable and possibly interfere with the functionality assays. It has shown for some methylated cyclodextrins to enhance the fluorescence signal of resorufin even though they evoke the loss of viability of those cells. This is due to the take up of these cyclodextrins via fluid-phase endocytosis.[74; 75] This raises the question whether this might be the case for other chemicals to have the same properties, resulting in the observed increase in fluorescence from section 4.7.4. Lactate is for example overly present in cell cultures where glycolysis is the main metabolic pathway, just as the methylated cyclodextrins it has a methyl group. If this was indeed the determining factor for an increase in fluorescence, this assay cannot be used to determine metabolic activity in these conditions.

Another considered explanation has to do with the released oxygen molecule of the resazurin, it was to be thought the oxygen might result in the aerobe metabolism to be activated, resulting in a higher degree of converting of resazurin, leading to a higher metabolic activity and thus more free oxygen. This is not the case, since this would be the same for all media, not only SFM, moreover a single oxygen molecule does not affect the aerobic metabolic properties of a cell, disproving this explanation.

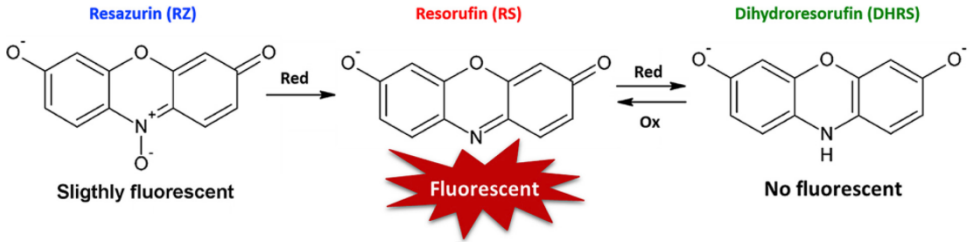

Figure 36: *Reaction of the slightly fluorescent resazurin into the highly fluorescent resorufin, adapted from Ibáñez et al.[76]*

Another substance which has been shown to interact with resazurin and result in the formation of resorufin, is ascorbic acid.[77] This can be explained by the fact that resazurin is in fact a redox indicator, so only indirectly does it indicate metabolic activity of a cell. If another component within the medium initiates redox reactions, this might be shown with resazurin and thus misinterpreted as high metabolic activity.
Although several explanations are thought of, it cannot yet be said as to which explanation is true, resulting in having to disregard PrestoBlue as an assay to determine metabolic activity in these experiments.

What can be concluded, is for both D72 and D86 to react in a similar way, whereas D302 often shows contradicting results. As to the medium used, the addition of ITS does indeed show improvement for cell survival compared to the conditions with SFM alone. The different coatings react quite similar, but it seems as if PD-coated surfaces do have a slightly more positive effect on cell count and metabolic activity than COL-coated surfaces.

4.8 Follow up

Since the best biological variables are defined, a chip can be loaded with this best combination of variables as a proof of concept for the functionality of this chip.

4.8.1 Proof of concept

Two octopus shaped outlet chips with long serpentine channels were coated with polydopamine, one seeded with D72 and one with D86 at a density of $2*10^4$ cells/cm^2. After the cell attachment, the chip was set up in a near anoxia environment and attached to the pump, filled with SFM+ITS, with one side enriched with 1 g/L glucose. Pictures of the chip were taken daily with an EVOS fluorescence microscope (Thermo Fisher, USA).

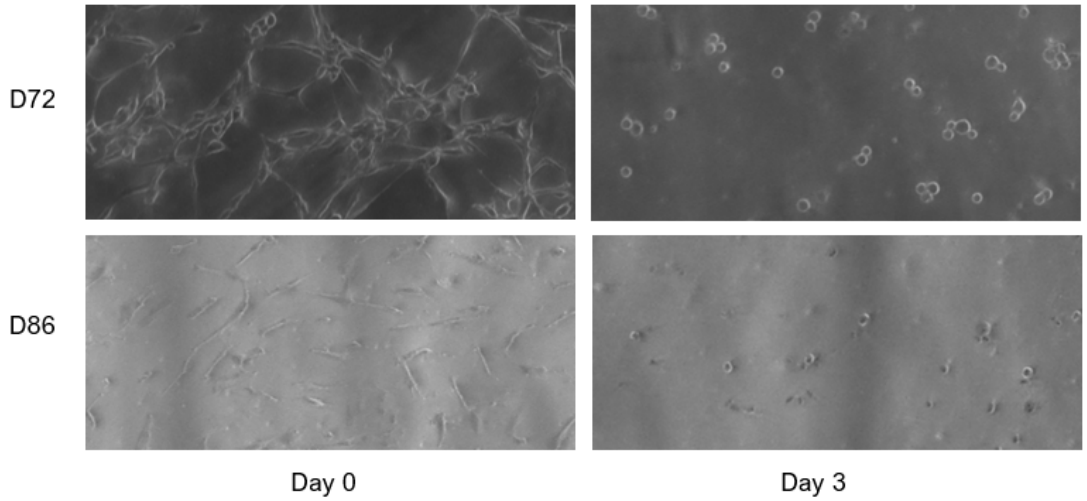

Figure 37: *PD-coated chips seeded with either D72 or D86, at day 0 and 3*

In the pictures of day 3, large morphological changes compared to day 0 are already observed. This suggests that eventhough the biological factores have been optimised, the flow still has a large effect on the cells, causing them to round up and detach.

From this it can concluded the biological factors are indeed of importance, but the effect of the flow rate has to still be taken into account. A possible solution for the cell detachment could be the use of a vastly slower flow rate within the chip.

4.8.2 Effect of flow rate

Two chips were coated with PD and seeded with a new donor (D138a), due to the lack of cells from the previous donors. These chips were exposed to a flow rate of 8.25 μL/min and 0.1375 μL/min, which comes down to a refreshment rate of the chambers once every minute and once every hour respectively. Pictures of the chip are taken daily with an EVOS fluorescence microscope (Thermo Fisher, USA) and a live/dead assay was performed at day 0 and day 7.

With the vastly slower flow rate of 0.1375 μL/min, the glucose availability for the cells comes down to 0,0833 ng/cell/min, still more than the theoretical static values of 3.8 pg/cell/min, but within the range of the observed glucose uptake in dynamic culture (4.57-133.87 pg/cell/min). The glucose uptake speed of the cells could have an effect on the glucose availability, which is why the system is attached to SFM+1 g/L glucose on both inlets. No ITS was added to the medium, since the tests were performed before recognising the beneficial effects of ITS on the cells' survival addition.

The pictures are shown in figure 38 where large morphological changes were expected between the condition with a refreshment rate of once every minute and once every hour, but both B and C seem

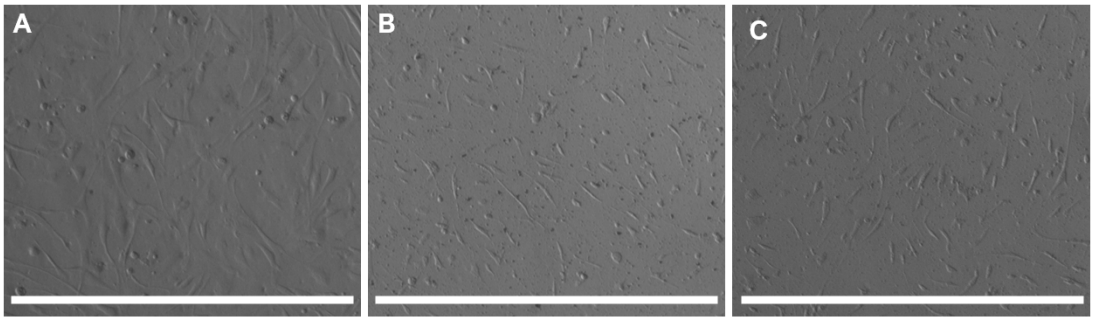

Figure 38: *Donor D138a at day 0 (A) and day 7 (B and C) at a refreshment rate of once every minute (B) and once every hour (C). Scale bar represents 1000µm in all pictures*

quite similar. Both exist of mainly elongated, stretched cells, but less wide than those at day 0. The live/dead assay shows similar results regarding percentage of live cells of the total culture at day 7, with 97,7% and 90,5% for a refreshment rate of once per minute and once per hour respectively. However, the cell count at day 7 vary greatly, as is shown in figure 39 this might be due to the vast decrease in glucose availability per minute. The decrease as opposed to day 0 can be due to the SFM and an increase would be expected to seen when looking at the results of the addition of ITS in section 4.7.4.

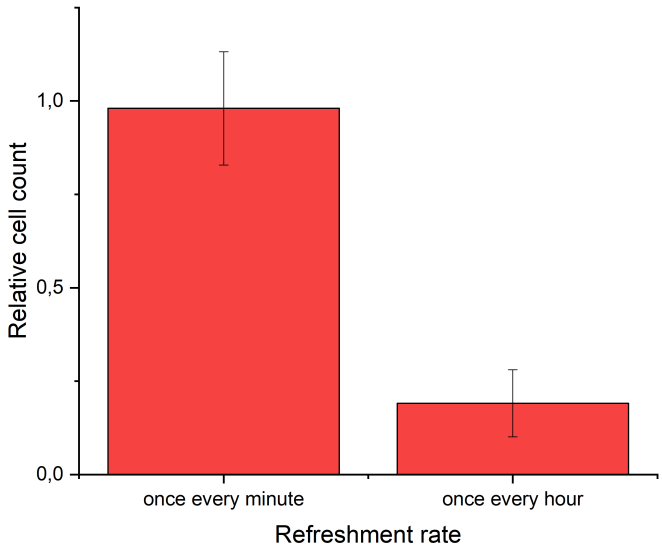

Figure 39: *Relative cell count as opposed to day 0 in a dynamic system with donor 138a with two different flow rates*

From this experiment and section 4.7.4 it can be concluded for the donor to have an immense impact on the viability and metabolic activity. Moreover it can be hypothesised for this donor (D138a) to perform in a more desirable way, compared to the previous 3 donors tested.

4.8.3 Determination of a proper donor

To go forward with this system, it is of utmost importance to identify a good donor before starting the tests with glucose gradients. One way to test this is by culturing different hMSCs donors side to side in aMEM in a static environment in normoxia and anoxia.

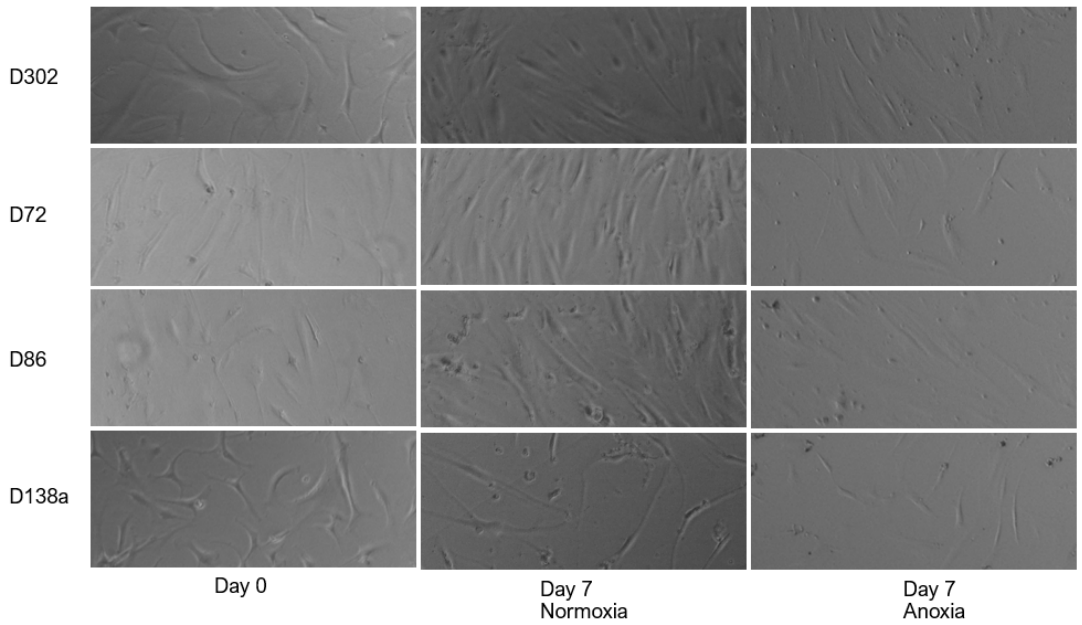

Figure 40: *Caption*

To test this, the 4 donors were seeded side to side and pictures were taken at day 0 and day 7, which can be seen in figure 40. When this method would be appropriate for determination of a proper donor, a difference would be shown between D138a and the other donors, since D138a has been shown to be functional in the chip.

Large variations between donors have been shown and the importance of choosing the right donor has been confirmed. The static experiments did not convincingly state the better donor, this might have been due to them functioning similarly in static conditions with aMEM. From purely observational standpoint, no conclusions can be drawn from this experiment. Confirming this method to not be sufficient for the determination of donor. Perhaps when restarting the same experiment with SFM or SFM+ITS, it could be determined which donor to be the best. So far the best method to determine which donor can be used for the experiment is by seeding the chip and applying flow.

5 Discussion

A dynamic culture system with several variables has been optimised, with all of the final choices displayed in table 6. However, several aspects have to be kept in mind when applying this system, such as the media used and the human variables within the system.

Design	Flow rate	8.25 uL/min/chip
	Outlet	Octopus shaped
	Channel length	Long
Tubing	Inner diameter	0.02 inch / 0.508 mm
	Attachment	Direct into the chip
	Material	Tygon microbore
	Filter	None
Biological factors	Seeding	Entire chip
	Coating	Polydopamine
	Medium	Serum free medium + Insulin-Transferrin-Selenium
	Donor	D138A

Table 6: *All optimised choices for all variables within the dynamic cell culture system*

5.1 Medium

5.1.1 Temperature

When the dynamic system is connected, the syringe, filled with medium, is kept at room temperature during the experiment which raises several questions. First of all the shelf life of medium depends on it being stored at 4°C, with the location of the medium being at room temperature this could negatively affect the medium stability. For cell culturing, medium is used of a temperature of 37°C, with it starting at room temperature, of about 22°C, a temperature change of 15°C will have to occur within the time it takes for the medium to flow through the tubing to the chip. The temperature of the medium entering the chip has however not been monitored, questioning to what extent the behaviour of the cells truly represents the *in vivo* environment.

5.1.2 Degree of solution

Another variable to take into account regarding the medium, is proper mixing and incorporation of all the components during the preparation of serum-free medium. When it is not mixed properly, it is possible for some components to not dissolve, which may lead to precipitation. Precipitation within a syringe could subsequently lead to a variable output, which affects the cellular behaviour and the conclusions drawn from the experiments.

5.2 Human variables

The optimisation of this system could not account for the remaining human factors, resulting in a not entirely fool-proof system. Two of these variables are handling the medium, which can result in bubbles, and the connection of the system, which can result in cell death and poor gradient.

5.2.1 Bubbles

Although the main cause for bubbles has been eliminated from the system, bubbles are still prone to form. It has been shown it is of utmost importance to remove all bubbles from the medium-filled syringes, but the level to which the bubbles are removed depends on the judgement of the executor. When a method can be created to accomplish a constant level of bubbles in the medium, as low as possible, it would most definitely improve the dynamic set up greatly.

5.2.2 Connecting the system

The other main human factor is the connection of all the components in this dynamic setup. As mentioned before, the tubing is manually inserted into the chip. Since the tubing fits very snug into the inlets and outlet, and due to the soft nature of the tubing material, pressure is needed to insert the tubing into the chip. However, when pressing the tubing too tightly, flow is obstructed which can result in a small bubble to form in the tubing. Moreover, when pushing the tubing too far into the chip, flow from the tubing towards the chip is obstructed, but when sticking it not far enough, it could disconnect over time due to pressure. Lastly, when pushing the tubing in too hard and pressing on the chip itself, the pressure could result in stress the cells observe, which can result in cell death.

5.2.3 Infections

Microfluidic chips on their own are very prone for infections, especially since these chips are not constructed in a sterile environment, the construction and translocation has to be executed carefully. With the system being partially in a non-sterile environment, caution has to be taken into account. Figure 13 shows the syringe, needle and tubing outside of the Xvivo LAF-cabinet, thus outside of the sterile environment. To maintain a set up as sterile as possible, the needles are attached to the tubing in a sterile site and closed with a filter. All of the tubing is entered through the cabinet, thoroughly cleaned and flushed through with ethanol, biocidal and PBS. The syringe is as well filled with medium in a sterile environment and closed off with a filter. This way all of the components are as sterile as possible, however the connection of the syringe to the tubing has to happen outside of this sterile environment, leading it to be a possible contamination site, prone to bringing in infections as is seen in figure 41

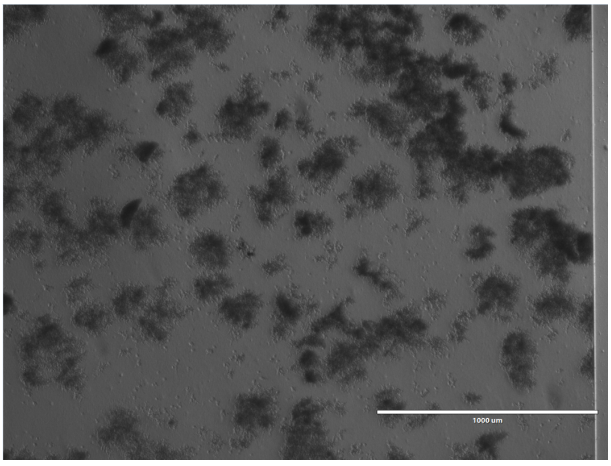

Figure 41: *Infection in the chip*

6 Conclusion

A gradient generating microfluidic system is optimised, for the quantification of the minimal metabolic requirements of hMSCs in near anoxia. Flow can be provided with a shear stress which does not negatively impact the cells. Polydopamine coated chips in combination with SFM supplemented with ITS seem to perform the best for this application. The system provides a stable gradient over time and allows for several metabolic concentrations to be fed through the system. Analysis can be performed on chip or via sampling, both during and at the and of the experiment, depending on the assay.

This is a promising suitable dynamic system, but caution has to be taken into account when using the system, since it is not fool-proof due to the human variables. Moreover, bubbles remain to stay a problem, so medium degassing and proper connectivity within the system is of utmost importance.

The wide variety between the donors' functionality has been described, underlining the importance of a good donor for the functionality of the dynamic system. The efficiency of a donor cannot be determined via morphology alone and most likely not solely via static tests either.

Several functionality assays can be used in combination with this system, but have to be optimised. PrestoBlue has shown to be a quick and easy assay for use in static conditions and on chip, but caution has to be taken when using this assay, since it has not yet been determined as to how it can result in extreme fluorescence in certain conditions.

Preliminary results show the gradient generating microfluidic system can be used to test multiple donors for multiple metabolite concentrations. With this system a data set can be constructed on the minimal metabolic requirements for hMSCs in anoxia and provide a stepping stone for future work with hMSCs regarding metabolism.

7 Recommendations

Since the aim of this project was to optimise a dynamic set up for the use of controlled nutrient supply for hMSCs in near anoxia, it is valuable to have a look at the next steps which have to be taken to apply this system for finding the minimal metabolic needs for hMSCs in near anoxia.

7.1 Set up

Currently the dynamic system is optimised to run for a maximum time of 8 days. To determine the effect of certain metabolic concentrations on hMSCs for longer periods of time, necessary to obtain true values of metabolic requirements for survival before an implant is attached to the donor site, the choice of pump will have to be reevaluated. The current standard PHD ULTRA CP syringe pump (Harvard Apparatus, USA), has a limit for the size of syringes which is 50 mL. This is the limiting factor for the run time, when expanding this time, a pump will have to be used which allows for larger syringes.

7.2 Donors

As has been discussed, a wide variety in hMSC response on the biological variables is observed. For this reason it is recommended to find a robust donor with which the first measurements on metabolic requirements are made. In section 4.8.3 it has been shown this determination can not be solely made on the basis of a purely morphological observations. The data from 4.7.4 was as well not convincing regarding the best donor, this could however have been due to the fact that none of those donors held up in a dynamic system. Since the most promising donor (D138a) has not been tested on its metabolic activity and viability in these circumstances, it can not yet be concluded this is not the best method to determine the best donor. For creating data on which further research can be based, it is recommended to build a data set with a wide variety of donors to gain a complete array on minimal metabolic needs.

7.3 Seeding methods

The current seeding method, where the entire chip is seeded as opposed to just the chambers, is shown to be functional. However, to eliminate as much variables form the system as possible, it would be favourable to find a method which successfully seeds the chip up until the end of the cell chambers. A seeding method that has been tried, but has not yet been successfully replicated, is to fill the entire chip with PBS and measure out the volume of cell suspension to be loaded in the chip to just fill the chambers. From the dimensions of the chip it is known the true volume of the chip up until the end of the cell chambers is 13.84 μL. However, when replicating this by filling the chip with micro beads via a syringe pump and tracking under a microscope, the volumes needed to fill the chambers vary widely from 6.07 μL to 18.98 μL. Moreover it was observed for the chambers to not fill evenly, but rather the outer chambers first and denser than the middle three chambers.

Another possibly successful method is to follow the current seeding method as described in section 4.6.1 but only partially coat the chip. This way, when seeding the chip, only the chambers and outlet will be hydrophilic and the serpentine channels will stay hydrophobic, resulting in attachment of the cells purely in the coated part of the chip. In section 4.5.1 it was shown the bare chip does not affect the glucose levels at the currently used flow rates. The possible downfall of this method is the difficulty to remove the bubbles trapped in the chip, due to its hydrophobicity.

7.4 Functionality assays

To assess the effect of glucose and other metabolic concentrations on the hMSCs, the aforementioned live/dead assay and PrestoBlue assays are used. For some functionality assays, volume would have to be extracted from each chamber. Several methods are attempted to extract the volume from the cell chambers, as is shown in figure 42.

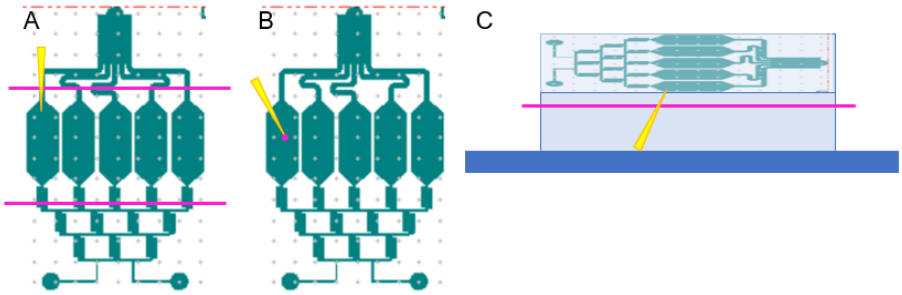

Figure 42: *Schematic representation of three methods assessed for extraction of the volume from the chip. Pink lines indicate cut lines and yellow arrows show the pipette tip used for extraction*

Via method A, the chip is cut open just above and below the cell chambers, after which the volume is carefully taken out of the cell chamber with a pipette. The volume can relatively easy be extracted from the chip, however, when cutting the PDMS the volume gets misplaced due to the pressure applied, leading to a mixture of the resulting volumes. With method B, it was tried to bypass this displacement of volume with carefully making a hole in the PDMS with a needle and take up the volume. Unfortunately the displacement still took place. The last method tried was method C, where the PDMS with the chip design was bonded on a flat PDMS surface, on top of a glass slide. The PDMS was cut just below the attachment point and the volume was taken up via the underside, but this method was not successful either. Going onward, functionality assays will have to be chosen on the possibility to execute them on chip, or just one concentration should flow through the chip, resulting in the outgoing flow to be used for assays.

7.4.1 Live/Dead assay

The live/dead assay provides the easiest, quickest, and most basal information about the cell culture. With this assay the bare minimum of glucose needs can be determined and a clear distinction between the concentration resulting in cell death and barely surviving cells is shown. However, when only focusing on this assay, the end result will be hMSCs which will barely be surviving. Cells on the verge of apoptosis are however not the most functional cells, since their priority is survival and not proliferation, which would be needed at the implant site.

7.4.2 PrestoBlue on chip

Since the PrestoBlue assay has thus far only been analysed using the Victor X3 Fluorescence plate reader (Thermo fisher, USA), a method has to be developed to assess the fluorescence of the medium in the chip. Since the volume in each chamber is too little for conventional analysis, it would be redundant to try and extract this volume from the chip.

The chips were fed with 10% PrestoBlue as with the static measurements and incubated for 30 minutes, after which they were analysed using a EVOS fluorescence microscope (Thermo Fisher, USA) with a DAPI filter by directly measuring the fluorescence from the chip and analysing using Fiji ImageJ software (Java, USA). The density profile is plotted and all values above half maximum were averaged and normalised against the chip with the highest average fluorescent value to find the percentage of the fluorescence intensity per chip. This method was tested with a PD-coated chip and COL-coated chip attached to flow with one concentration of glucose over the entire chip in normoxia, a PD-coated chip without flow, all seeded with 3T3 cells in dMEM and an empty chip without cells as control.

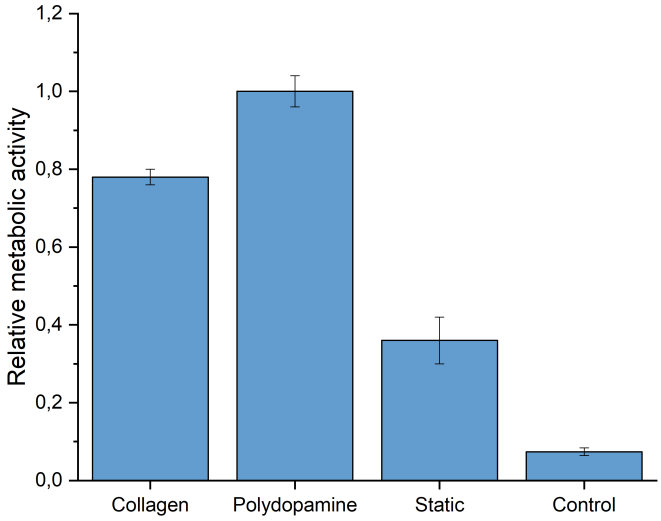

Figure 43: *Analysis of PrestoBlue on chip, measured with 3T3s in a COL-coated chip, PD-coated chip, PD-coated chip without flow and an empty control chip.*

In figure 43 the relative metabolic activity is shown of each condition. From this graph it can be concluded the relative metabolic activity can be assessed via a PrestoBlue on chip, since clear differences as a result of different metabolic activities of the cell cultures are observed.

Although PrestoBlue is often used as an assay for determination of metabolic activity, it has been shown in section 4.7.4 to not be a reliable analysis when used for cell cultures in SFM. It does seem to provide proper analysis for SFM+ITS, but to eliminate possible misinterpreted readouts different functionality assay for the cause of analysing metabolic activity of the cell should be considered.

7.4.3 VEGF production

One way to asses the cells' metabolic activity, is to measure the VEGF production. Upregulation of HIF-1a due to oxygen deficiency leads to an increase in VEGF production.[78] The VEGF levels within a cell culture in combination with the cell count can provide information regarding the level of activity of the cell.

To perform these measurements, samples of the medium will have to be taken at each cell chamber since different glucose concentrations result in different VEGF levels. This is however not possible for this chip design as mentioned before, so to still assess the cells' functionality with VEGF, a chip can be connected to just one concentration of medium, so the output volume can measured for its VEGF levels.

7.4.4 qPCR

Metabolic activity and a live/dead assay do not provide a complete view on the true functionality of the cell culture. Several other factors are of interest such as cell cycle, aerobe and glucose respiratory, differentiation potential, and the cells' susceptibility for apoptosis. To gain information on these factors, a qPCR can be performed with primers for these specific characteristics.

With information gained from these assays, a more complete dataset can be determined with a wide array of data from the concentration at which cells barely survive towards the minimal concentration needed for the cells to still be fully functional.

7.5 Metabolites

Currently, glucose is the only metabolite looked at, this is however not the only metabolite taken up by the cells the *in vivo* environment. With the presentation of an array of multiple metabolites, a more beneficial response is expected. With a certain mixture of different concentrations of metabolites certain desired responses might be triggered, which can be used to our advance. Although it is known for stem cells to rely mainly on glycolysis for their energy source, it is worth it to look into other metabolites for their possible added value.[79]To determine which metabolites are of interest, the anaerobic metabolic pathways are looked into.

7.5.1 Glutamine

Glutamine is the most common amino acid in the plasma and plays a role in a variety of biochemical functions. The most important role being its function as a primary metabolic fuel for proliferating cells. Furthermore, glutamine can be used as an alternative input for the TCA cycle to support ATP production or as a source of citrate for fatty acid synthesis in actively proliferating cells. This alternative input for the TCA cycle is of need due to it mainly running as a result of oxygen. When offering glutamine directly to the cell, this oxygen dependency could possibly be bypassed.

In the absence of constant replenishment, essential amino acids will be rapidly depleted in vascular compromised tissues, causing a problem for cell proliferation. [41; 80]

In anoxia glutamine is of importance for its delivery of metabolites to the TCA cycle. Glutamine uptake is increased by hypoxic conditions, switching its fate from a oxidative pathway to the reductive carboxylation pathway, which is responsible to convert glutamine into citrate.[43] Moreover, it has been shown for glutamine to be degraded to lactate, in this process NADPH is generated, which supplies other anabolic processes.[81]

Lastly, glutamine is a precursor for α-ketoglutarate, which causes increasing levels of proliferation, ECM accumulation, and α-ketoglutarate leads to a decrease in ammonia toxicity, enhancing batch-culture survival.[82; 83; 84] With the addition of glutamine to the medium, it is expected for the cells to demonstrate increased proliferation and survival.

7.5.2 R5P

The pentose phosphate pathway generates ribose-5-phosphate (R5P), an important intermediate metabolite since it is a substrate for purine synthesis. The concentration of R5P is a determining factor of the purine synthesis rate. Purines have many functions but are mostly important for the production of nucleotides and nucleic acids, act as metabolic signals, and control cell growth.[85; 86; 87]

R5P is a result from glucose 6-phosphate (G6P), an intermediate from the glycolysis. Due to the hypoxic environment, R5P cannot be created via G6P, since this occurs in the oxidative branch of the PPP.[88] With the addition of R5P to the medium for the cell culture in anoxia, it is expected to positively affect the cell growth.

Moreover, metabolites play a role in differentiation potential of stem cells and numerous studies have shown adjustment in metabolite availability of a single metabolite to be able to dramatically impact a stem cells' fate.[89] After finding the minimal metabolic needs of the combination of glucose, glutamine, and R5P, it is suggested to determine metabolites with a decisive role in differentiation towards the desired tissue.

7.6 Future applications

With the optimisation of this set up, a data set can be constructed with the minimal metabolic needs for stem cells to be functional in near-anoxia. With this data, hMSCs in an implant of sufficient size could be supplied with the right amount of nutrients. This addition of nutrients is likely to increase cell survival in the implants, giving rise to a new challenge, the controlled release of these nutrients into the cellular environment.

When this release of nutrients does not occur in a controlled way but rather all at once, it can not be ensured for the cells to survive the calculated time span. This is a result of the minimal needs being lower than the desired levels of nutrients. When this challenge of controlled release is overcome, the implementation of nutrients within an implant could play a key role with the scale up of tissue engineered constructs. The nutrient supply could as well be combined with a vascularized construct, realising short term survival of hMSCs, while vascularization of the construct is being connected to the implant site.

References

[1] O'Brien. Biomaterials scaffolds for tissue engineering. Biomaterials. 2011 March;14(3):88–95.

[2] Kim KT, Eo MY, Nguyen TTH, Kim SM. General review of titanium toxicity. International journal of implant dentistry. 2019;5(1):1–12.

[3] Green B, Griffiths E, Almond S. Neuropsychiatric symptoms following metal-on-metal implant failure with cobalt and chromium toxicity. Bmc Psychiatry. 2017;17(1):1–5.

[4] Goldberg VM. Natural history of autografts and allografts. Bone implant grafting. 1992;p. 9–12.

[5] Giannoudis PV, Dinopoulos H, Tsiridis E. Bone substitutes: an update. Injury. 2005;36(3):S20–S27.

[6] van Blitterswijk, de Boer. Tissue engineering, second edition;.

[7] Poser L, Matthys R, Schawalder P, Pearce S, Alini M, Zeiter S. A Standardized Critical Size Defect Model in Normal and Osteoporotic Rats to Evaluate Bone Tissue Engineered Constructs. BioMed Research International. 2014;(2014):348635.

[8] Yang G, Mahadik B, Choi JY, Fisher JP. Vascularization in tissue engineering: fundamentals and state-of-art. Progress in Biomedical Engineering. 2020;2:012002.

[9] Wu I, Elisseeff J. Biomaterials and tissue engineering for soft tissue reconstruction. In: Natural and Synthetic Biomedical Polymers. Elsevier; 2014. p. 235–241.

[10] Ren X, Zhao M, Lash B, Martino MM, Julier Z. Growth Factor Engineering Strategies for Regenerative Medicine Applications. Frontiers in Bioengineering and Biotechnology;7.

[11] Squillaro T, Peluso G, Galderisi U. Clinical Trials With Mesenchymal Stem Cells: An Update. Cell Transplant. 2016;25(5):829–848.

[12] Han Y, Li X, Zhang Y, Han Y, Chang F, Ding J. Mesenchymal Stem Cells for Regenerative Medicine. Cells. 2019 August;8(8):886.

[13] Galipeau J, Sensébé L. Mesenchymal Stromal Cells: Clinical Challenges and Therapeutic Opportunities. Cell Stem Cell. 2018 June;22(6):824–833.

[14] Ferro F, Spelat R, G S, Duffy N, Islam MN, O'Shea PM, et al. Survival/Adaptation of Bone Marrow-Derived Mesenchymal Stem Cells After Long-Term Starvation Through Selective Processes. STEM CELLS. 2019 March;37(6):813–827.

[15] Hofer HR, Tuan RS. Secreted trophic factors of mesenchymal stem cells support neurovascular and musculoskeletal therapies. Stem Cell Research Therapy. 2016 September;7(1):1–14.

[16] Rouwkema J, Rivron NC, van Blitterswijk CA. Vascularization in tissue engineering. Trends in Biotechnology. 2008 June;26(8):434–441.

[17] Novosel EC, Kleinhans C, Kluger PJ. Vascularization is the key challenge in tissue engineering. Advanced drug delivery reviews. 2011;63(4-5):300–311.

[18] Sloff M, de Vries R, Geutjes P, IntHout J, Ritskes-Hoitinga M, Oosterwijk E, et al. Tissue Engineering in Animal Models for Urinary Diversion: A Systematic Review. PLoS One. 2014 June;9(6):e98734.

[19] Lee YS, Cho SY, Kim HW, Kang SH, Kim HY, Lee JY, et al. Preliminary Study of Tissue-Engineered Ileal Conduit Using Poly (ε-Caprolactone) (PCL) Nano-Sheet Seeded with Muscle-Derived Stem Cells. Korean Journal of Urology. 2009 March;50(3):282–287.

[20] Oryan A, Alidadi S. Reconstruction of radial bone defect in rat by calcium silicate biomaterials. Life sciences;201.

[21] Zeiter S, Koschitzki K, Alini M, Jakob F, Rudert M, Herrmann M. Evaluation of Preclinical Models for the Testing of Bone Tissue-Engineered Constructs. Tissue Engineering Part C: Methods. 2020 February;26(2):107–117.

[22] Place TL, Domann F, Case A. Limitations of oxygen delivery to cells in culture: An underappreciated problem in basic and translational research. Free radical biology medicine. 2017;113:311–322.

[23] Kwon H, Brown WE, Lee CA, Wang D, Paschos N, Hu JC, et al. Surgical and tissue engineering strategies for articular cartilage and meniscus repair. Nature Reviews Rheumatology. 2019 July;15(9):550–570.

[24] Rouwkema J, Koopman B, Blitterswijk CA, Dhert W, Malda J. Supply of nutrients to cells in engineered tissues. Biotechnology Genetic engineering reviews;26.

[25] Malda J, Rouwkema J, Martens DE, le Comte EP, Kooy FK, Tramper J, et al. Oxygen gradients in tissue-engineered Pegt/Pbt cartilaginous constructs: Measurement and modeling. Biotechnology and Bioengineering. 2004 February;86(1):9–18.

[26] Kathagen A, Schulte A, Balcke G, Phillips HS, Martens T, Matschke J, et al. Hypoxia and oxygenation induce a metabolic switch between pentose phosphate pathway and glycolysis in glioma stem-like cells. Acta Neuropathologica. 2013 September;126(5):763–780.

[27] Widowati W, Wijaya L, Bachtiar I, Gunanegara RF, Sugeng SU, Irawan YA, et al. Effect of oxygen tension on proliferation and characteristics of Wharton's jelly-derived mesenchymal stem cells. Biomarkers and Genomic Medicine. 2014 March;6(1):43–48.

[28] Lalu MM, McIntyre L, Pugliese C, Fergusson D, Winston BW, Marshall JC, et al. Safety of cell therapy with mesenchymal stromal cells (SafeCell): a systematic review and meta-analysis of clinical trials. PLoS One. 2012 October;7(10):e47559.

[29] Karnieli O, Friedner OM, Allickson JG, Zhang N, Jung S, Fiorentini D, et al. A consensus introduction to serum replacements and serum-free media for cellular therapies. Cytotherapy. 2017 February;19(2):155–169.

[30] Eelen G, Treps L, Li X, Carmeliet P. Basic and Therapeutic Aspects of Angiogenesis Updated. Circulation Research. 2020 July;127(3):310–329.

[31] Alberts B, Johnson A, Lewis J, Raff M, Roberts K, Walter P. Molecular Biology of the Cell, 4th edition. Garland Science;.

[32] Reddy LVK, Murugan D, Mullick M, Moghal ETB, Sen D. Recent Approaches for Angiogenesis in Search of Successful Tissue Engineering and Regeneration. Current Stem Cell Research Therapy. 2020;15(2):111–134.

[33] Willemen NGA, Hassan S, Gurian M, Li J, Allijn IE, Shin SR, et al. Oxygen-Releasing Biomaterials: Current Challenges and Future Applications. Trends in Biotechnology;.

[34] Lu Z, Jiang X, Chen M, Feng L, Kang YJ. An oxygen-releasing device to improve the survival of mesenchymal stem cells in tissue engineering. Biofabrication. 2019;11(4):045012.

[35] Camci-Unal G, Alemdar N, Annabi N, Khademhosseini A. Oxygen Releasing Biomaterials for Tissue Engineering. Polymer International. 2013 June;62(6):843–848.

[36] Newland H, Eigel D, Rosser A, Werner C, Newland B. Oxygen producing microscale spheres affect cell survival in conditions of oxygen-glucose deprivation in a cell specific manner: implications for cell transplantation. Biomaterials science. 2018;6(10):2571–2577.

[37] Deschepper M, Oudina K, David B, Myrtil V, Collet C, Bensidhoum M, et al. Survival and function of mesenchymal stem cells (MSCs) depend on glucose to overcome exposure to long-term, severe and continuous hypoxia. Journal of cellular and molecular medicine. 2011;15(7):1505–1514.

[38] Moya A, Paquet J, Deschepper M, Larochette N, Oudina K, Denoeud C, et al. Human mesenchymal stem cell failure to adapt to glucose shortage and rapidly use intracellular energy reserves through glycolysis explains poor cell survival after implantation. Stem Cells. 2018;36(3):363–376.

[39] Nuschke A, Rodrigues M, Wells AW, Sylakowski K, Wells A. Mesenchymal stem cells/multipotent stromal cells (MSCs) are glycolytic and thus glucose is a limiting factor of in vitro models of MSC starvation. Stem cell research & therapy. 2016;7(1):1–9.

[40] Fan Y, Zong W. The cellular decision between apoptosis and autophagy. Chinese Journal of Cancer. 2013 March;32(3):121–129.

[41] O'Neill LAJ, Kishton RJ, Rathmell J. A guide to immunometabolism for immunologists. Nature Reviews Immunology;16.

[42] D Huang CL, Zhang H. Hypoxia and cancer cell metabolism. Acta Biochimica et Biophysica Sinica. 2014 March;46(3):214–219.

[43] Yoo HC, Yu YC, Sung Y, Han JM. Glutamine reliance in cell metabolism. Experimental Molecular Medicine. 2020 September;52(9):1496–1516.

[44] Chinopoulos C. Which Way Does the Citric Acid Cycle Turn During Hypoxia? The Critical Role of a-Ketoglutarate Dehydrogenase Complex. Journal of neuroscience research. 2013;91(8):1030–1043.

[45] Choudhry H, Harris AL. Advances in Hypoxia-Inducible Factor Biology. Cell Metabolism. 2018 February;27(2):281–298.

[46] Sackmann EK, Fulton AL, Beebe DJ. The present and future role of microfluidics in biomedical research. Nature;507.

[47] Mehling M, Tay S. Microfluidic cell culture. Current Opinion in Biotechnology;25.

[48] Li Z, Venkataraman A, Rosenbaum MA, Angenent LT. A Laminar-Flow Microfluidic Device for Quantitative Analysis of Microbial Electrochemical Activity. Chemistry-Sustainability-Energy-Materials;5.

[49] Jeon NL, Dertinger SKW, Chiu DT, Choi IS, Stroock AD, Whitesides GM. Generation of Solution and Surface Gradients Using Microfluidic Systems. Langmuir. 2000 October;16(22):8311–8316.

[50] Bulutoglu B, Rey-Bedón C, Kang YBA, Mert S, Yarmush ML, Usta OB. A microfluidic patterned model of non-alcoholic fatty liver disease: applications to disease progression and zonation. Lab on a Chip. 2019;19(18):3022–3031.

[51] Glossop JR, Cartmell SH. Effect of fluid flow-induced shear stress on human mesenchymal stem cells: differential gene expression of IL1B and MAP3K8 in MAPK signaling. Gene Expression Patterns. 2009;9(5):381–388.

[52] Arora S, Srinivasan A, Leung CH, Toh Y. Bio-mimicking Shear Stress Environments for Enhancing Mesenchymal Stem Cell Differentiation. Current Stem Cell Research and Therapy. 2020;15(5):414–427.

[53] Stone SD, Hollins BC. Modeling Shear Stress in Microfluidic Channels for Cellular Applications. In: 2013 29th Southern Biomedical Engineering Conference. IEEE; 2013. p. 117–118.

[54] Z Wu NN, Huang X. Nonlinear diffusive mixing in microchannels: Theory and experiments. J Micromech Microeng. 2004 04;14:604–611.

[55] Wang J, Chen W, J Sun J, Liu C, Yin Q, Zhang L, et al. A microfluidic tubing method and its application for controlled synthesis of polymeric nanoparticles. Lab on a Chip. 2014;14(10):1673–1677.

[56] Marturano-Kruik A, Nava MM, Yeager K, Chramiec A, Hao L, Robinson S, et al. Human bone perivascular niche-on-a-chip for studying metastatic colonization. Proceedings of the National Academy of Sciences. 2018;115(6):1256–1261.

[57] Zhang W, Zhang YS, Bakht SM, Aleman J, Shin SR, Yue K, et al. Elastomeric free-form blood vessels for interconnecting organs on chip systems. Lab on a Chip. 2016;16(9):1579–1586.

[58] Saint-Gobain. Tygon-nd-100-80-datasheet;. `https://www.medical.saint-gobain.com/`.

[59] Pereiro I, Khartchenko AF, Petrini L, Kaigala GV. Nip the bubble in the bud: a guide to avoid gas nucleation in microfluidics. Lab on a chip. 2019 June;19(14):2296–2314.

[60] Lee H, Dellatore S, Miller W, Messersmith P. Mussel-inspired surface chemistry for multifunctional coatings. Science. 2007 October;318(5849):426–430.

[61] Kanitthamniyom P, Zhang Y. Application of polydopamine in biomedical microfluidic devices. Microfluidics and Nanofluidics. 2018 February;22(3):1–13.

[62] Simple surface engineering of polydimethylsiloxane with polydopamine for stabilized mesenchymal stem cell adhesion and multipotency. Scientific reports. 2015;5(1):1–12.

[63] Li Q, Rycaj K, Chen X, Tang D. Cancer stem cells and cell size: A causal link? Seminars in cancer biology;35.

[64] Viguet-Carrin S, Garnero P, Delmas P. The role of collagen in bone strength. Osteoporosis international. 2006;17(3):319–336.

[65] Razavi M, Hu S, Thakor AS. A collagen based cryogel bioscaffold coated with nanostructured polydopamine as a platform for mesenchymal stem cell therapy. Journal of Biomedical Materials Research Part A. 2018 April;106(8):2213–2228.

[66] Marino G, Niso-Santano M, Baehrecke EH, Kroemer G. Self-consumption: the interplay of autophagy and apoptosis. Nature reviews Molecular cell biology. 2014;15(2):81–94.

[67] Zhu W, Chen J, Cong X, Hu S, Chen X. Hypoxia and serum deprivation-induced apoptosis in mesenchymal stem cells. Stem cells. 2006;24(2):416–425.

[68] Liu X, Zhang T, Wang R, Shi P, Pan B, Pang X. Insulin-Transferrin-Selenium as a Novel Serum-free Media Supplement for the Culture of Human Amnion Mesenchymal Stem Cells. Annals of Clinical Laboratory Science. 2019;49(1):63–71.

[69] Sato Y, Endo H, Okuyama H, Yamagata K, Shimomura I, Inoue M. Cellular hypoxia of pancreatic beta-cells due to high levels of oxygen consumption for insulin secretion in vitro. Journal of biological chemistry. 2011 April;286(14):12524–12532.

[70] Baker RD, Baker SS, Rao R. Selenium deficiency in tissue culture: implications for oxidative metabolism. Journal of pediatric gastroenterology and nutrion. 1998 October;27(4):387–392.

[71] Trivedi A, Miyazawa B, Gibb S, Valanoski K, Vivona L, Lin M, et al. Bone marrow donor selection and characterization of MSCs is critical for pre-clinical and clinical cell dose production. Journal of translational medicine. 2019;17(1):1–16.

[72] Chen JL, Steele TWJ, Stuckey DC. Metabolic reduction of resazurin; location within the cell for cytotoxicity assays. Biotechnology and Bioengineering. 2018 February;115(2):351–358.

[73] Zhang H, Du G, Zhang J. Assay of mitochondrial functions by resazurin in vitro. Acta Pharmacologica Sinica. 2004 March;25(3):385–389.

[74] Csepregi R, Lemli B, Kunsági-Máté S, andT Kőszegi LS, Németi B, Poór M. Complex Formation of Resorufin and Resazurin with B-Cyclodextrins: Can Cyclodextrins Interfere with a Resazurin Cell Viability Assay? Molecules. 2018 382;23(2).

[75] Fenyvesi F, Réti-Nagy K, Bacsó Z, Gutay-Tóth Z, Malanga M, Fenyvesi [U+FFFD] et al. Fluorescently Labeled Methyl-Beta-Cyclodextrin Enters Intestinal Epithelial Caco-2 Cells by Fluid-Phase Endocytosis. PLoS one. 2014 January;9(1):e84856.

[76] Ibáñez D, Izquierdo-Bote D, Pérez-Junquera A, González-García MB, Hernández-Santos D, Fanjul-Bolado P. Raman and fluorescence spectroelectrochemical monitoring of resazurin-resorufin fluorogenic system. Dyes and Pigments. 2020 January;172:107848.

[77] Wang F, Li Y, Li W, Zhang Q, Chen J, Zhou H, et al. A facile method for detection of alkaline phosphatase activity based on the turn-on fluorescence of resorufin. Analytical Methods. 2014;6(15):6105–6109.

[78] Jham BC, Ma T, Hu J, Chaisuparat R, Friedman ER, Pandolfi PP, et al. Amplification of the Angiogenic Signal through the Activation of the TSC/mTOR/HIF Axis by the KSHV vGPCR in Kaposi's Sarcoma. PLoS one. 2011 April;6(4):e19103.

[79] Mathieu J, Zhou W, Xing Y, Sperber H, Ferreccio A, Agoston Z, et al. Hypoxia-Inducible Factors Have Distinct and Stage-Specific Roles during Reprogramming of Human Cells to Pluripotency. Cell stem cell. 2014;14(5):592–605.

[80] Green DR, Galluzzi L, Kroemer G. Metabolic control of cell death. Science;345(6203).

[81] DeBerardinis RJ, Mancuso A, Daikhin E, Nissim I, Yudkoff M, Wehrli S, et al. Beyond aerobic glycolysis: transformed cells can engage in glutamine metabolism that exceeds the requirement for protein and nucleotide synthesis. Proceedings of the National Academy of Sciences. 2007;104(49):19345–19350.

[82] Singh D, Vishnoi T, Kumar A. Effect of Alpha-Ketoglutarate on Growth and Metabolism of Cells Cultured on Three-Dimensional Cryogel Matrix. International journal of biological sciences. 2013;9(5):521.

[83] MacKenzie E, Selak M, Tennant D, Payne LJ, Crosby S, Frederiksen CM, et al. Cell-Permeating α-Ketoglutarate Derivatives Alleviate Pseudohypoxia in Succinate Dehydrogenase-Deficient Cells. Molecular and Cellular Biology. 2007;27(9):3282–3289.

[84] Dang CV. Links between metabolism and cancer. Genes & development. 2012;26(9):877–890.

[85] for Biotechnology Information NC. PubChem Compound Database;.

[86] Fumagalli M, Lecca D, Abbracchio MP, Ceruti S. Pathophysiological Role of Purines and Pyrimidines in Neurodevelopment: Unveiling New Pharmacological Approaches to Congenital Brain Diseases. Frontiers in Pharmacology;8.

[87] Love NR, Ziegler M, Amaya YCE. Carbohydrate metabolism during vertebrate appendage regeneration: What is its role? How is it regulated? Bioessays. 2014;36(1):27–33.

[88] Bertels LK, Murillo LF, Heinisch JJ. The Pentose Phosphate Pathway in Yeasts–More Than a Poor Cousin of Glycolysis. Biomolecules. 2021;11(5):725.

[89] Tsogtbaatar E, Landin C, Minter-Dykhouse K, Folmes CDL. Energy metabolism regulates stem cell pluripotency. Frontiers in cell and developmental biology. 2020;8:87.

A Supplementary

A.1 Measurements chip

Figure 44 shows the measurements of the chip design octopus shaped outlet and long serpentine channels.

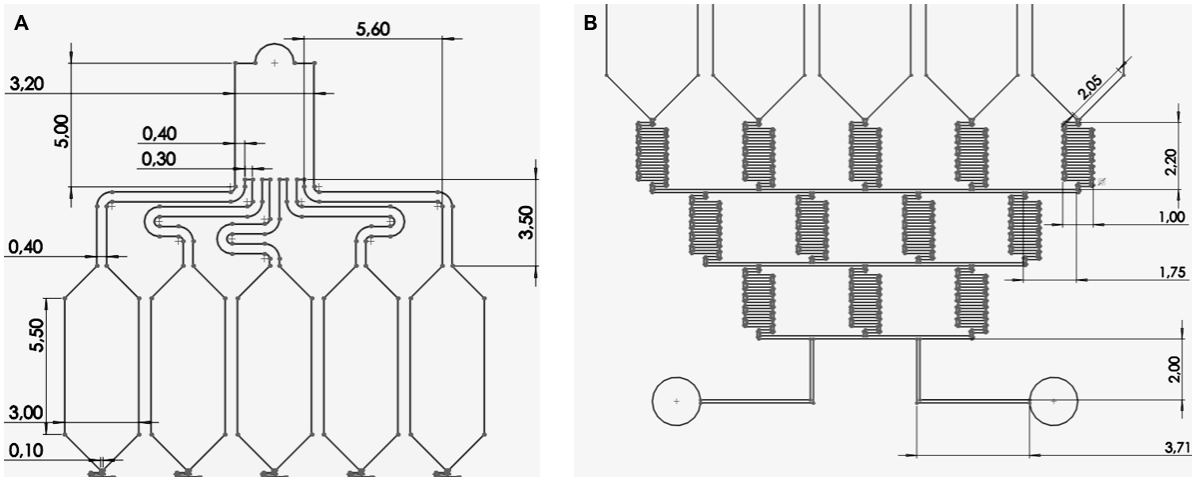

Figure 44: *Measurements of A) the top part and B) bottom part of the chip design with octopus shaped outlet and long serpentine channels*

A.2 Optimisation of biological variables

All of the conditions of the static experiment for determination of the best combinations of variables are shown in the table below.

	aMEM			SFM			SFM+ITS		
D72	D72	PD	aMEM	D72	PD	SFM	D72	PD	SFM+ITS
	D72	COL	aMEM	D72	COL	SFM	D72	COL	SFM+ITS
	D72	Cntrl	aMEM	D72	Cntrl	SFM	D72	Cntrl	SFM+ITS
D86	D86	PD	aMEM	D86	PD	SFM	D86	PD	SFM+ITS
	D86	COL	aMEM	D86	COL	SFM	D86	COL	SFM+ITS
	D86	Cntrl	aMEM	D86	Cntrl	SFM	D86	Cntrl	SFM+ITS
D302	D302	PD	aMEM	D302	PD	SFM	D302	PD	SFM+ITS
	D302	COL	aMEM	D302	COL	SFM	D302	COL	SFM+ITS
	D302	Cntrl	aMEM	D302	Cntrl	SFM	D302	Cntrl	SFM+ITS

A.2.1 Change in color with PrestoBlue

The extreme values of section 4.7.4 were observed before measuring the fluorescence. The change of color was clearly visible, it changed from a dark blue to a bright pink, as is seen in figure 45.

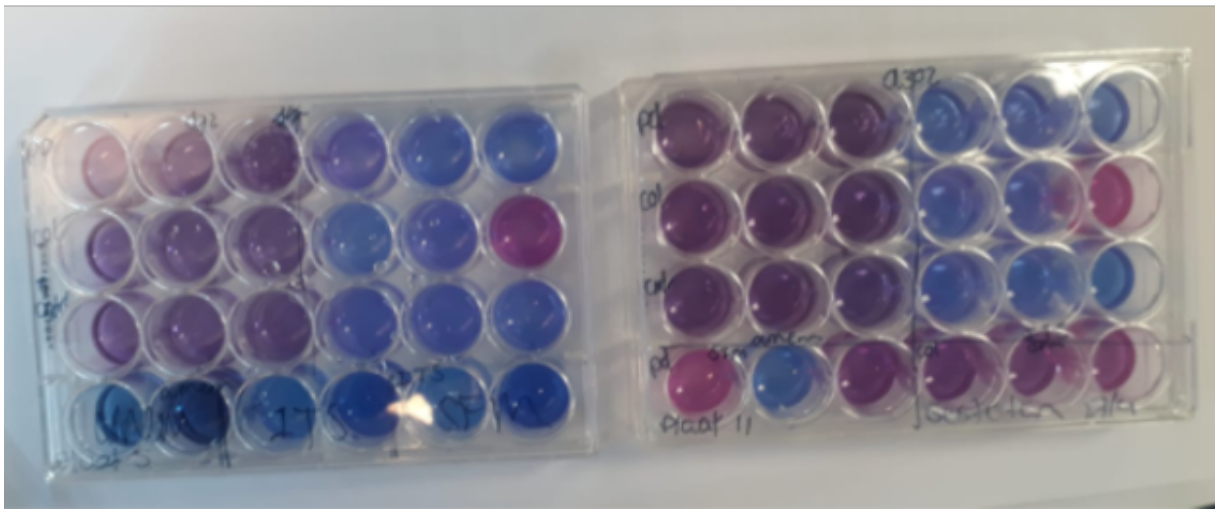

Figure 45: *Picture of two 24-wells plate at day 7 after performing a PrestoBlue assay*